PB-215 171

MODEL STUDIES OF OUTFALL SYSTEMS FOR DESALINATION PLANTS. PART III. NUMERICAL SIMULATION AND DESIGN CONSIDERATIONS

M. A. Zeitoun, et al

Dow Chemical Company

Prepared for:

Office of Saline Water

December 1972

MODEL STUDIES OF OUTFALL SYSTEMS FOR DESALINATION PLANTS

PART III
NUMERICAL SIMULATION AND DESIGN CONSIDERATIONS

United States Department of the Interior

Office of Saline Water . Research and Development Progress Report No. 804

Int-OSW-RDPR-72-804

SELECTED WATER RESOURCES ABSTRACTS
INPUT TRANSACTION FORM

1. Report No. 804 | 2. | 3. Accession No. W

4. Title Model Studies of Outfall Systems for Desalting Plants (Part III - Numerical Simulation & Design Considerations)

5. Report Date Dec. 1972
6.
8. Performing Organization Report No.

7. Author(s) M. A. Zeitoun, R. O. Reid, Texas A&M
W. F. McIlhenny, T. M. Mitchell, Texas A&M

10. Project No. OSW R&D Prog. Report No. 804

9. Organization Dow Chemical Co.
Freeport, Texas

11. Contract/Grant No. 14-01-0001-2169, Amdt. 2

13. Type of Report and Period Covered R&D
Apr. '70 - Feb. '72

12. Sponsoring Organization Office of Saline Water

15. Supplementary Notes
Office of Saline Water Research & Development Progress Report No.

16. Abstract: Although at coastal locations, the saline dense effluent from a desalting plant is potentially harmful to the marine organisms, the environmental effects can be minimized or eliminated if the effluent is properly mixed with and diluted by the receiving water.

Conceptual designs of outfall systems were previously developed on the basis of laboratory tests and are presented in OSW R&D Progress Report No. 550.

Experimental verification of the conceptual designs by the U. S. Army Corps of Engineers was published as Parts I and II of this report (R&D Nos. 714 and 736).

The data obtained in the flume study were used to calibrate several existing models for the jet regime. The model chosen gives a reasonable simulation of the geometry of the jet axis and the dilution at the peak of the jet, but was found to oversimulate the lateral spreading factor.

Application of equations to the design of diffusers is presented. Numerical simulation of the dispersion of a dense effluent discharge into a homogeneous stream is included.

17a. Descriptors *Brine disposal, *model studies, desalination plants, effluents, outlets, waste disposal

17b. Identifiers *Marine ecology, *Effluent dispersion, Diffusers, Model flume, Outfall Designs

17c. COWRR Field & Group 05E

18. Availability NTIS

19. Security Class. (Report) Unclassified

20. Security Class. (Page)

21. No. of Pages 87

22. Price $3.00-0.95

Send To: WATER RESOURCES SCIENTIFIC INFORMATION CENTER
U.S. DEPARTMENT OF THE INTERIOR
WASHINGTON, D. C. 20240

Abstractor C. L. Grantee

Institution Offc. of Saline Water, U. S. Dept. of Inter.

Research and Development Progress Report No.804 December 1972
Int-OSW-RDPR-72-804

MODEL STUDIES OF OUTFALL SYSTEMS FOR DESALINATION PLANTS

PART III
NUMERICAL SIMULATION AND DESIGN CONSIDERATIONS

By Dr. M. A. Zeitoun, Mr. W. F. McIlhenny, Dow Chemical Company, Freeport, Texas; R. O. Reid and T. M. Mitchell, Texas A & M University, College Station, Texas; for Office of Saline Water, J. W. O'Meara, Director; W. F. Savage, Assistant Director, Engineering & Development; W. W. Rinne, Chief, Special Projects Division; C. L. Gransee, Project Engineer.

Contract No. 14-01-0001-2169

UNITED STATES DEPARTMENT OF THE INTERIOR . Rogers C. B. Morton, Secretary
James R. Smith, Assistant Secretary, Water and Power Resources

As the Nation's principal conservation agency, the Department of the Interior has basic responsibilities for water, fish, wildlife, mineral, land, park, and recreational resources. Indian Territorial affairs are other major concerns of America's "Department of Natural Resources".

The Department works to assure the wisest choice in managing all our resources so each will make its full contribution to a better United States—now and in the future.

FOREWORD

This is one of a continuing series of reports designed to present accounts of progress in saline water conversion and the economics of its application. Such data are expected to contribute to the long-range development of economical processes applicable to low-cost demineralization of sea and other saline water.

Except for minor editing, the data herein are as contained in a report submitted by the contractor. The data and conclusions given in the report are essentially those of the contractor and are not necessarily endorsed by the Department of the Interior.

TABLE OF CONTENTS

Section		Page
I.	Introduction.	1
II.	Summary and Conclusions	8
III.	Numerical Simulation of the Dispersion of a Dense Effluent Discharged Into a Homogeneous Stream (Texas A & M).	10
	A. Introduction.	10
	B. Comparison of Some Existing Models for the Jet Regime in a Cross-Stream. .	13
	C. Model Chosen for the Present Study of the Dense Jet Regime	18
	D. Non-Dimensional Form of the Model . . .	19
	E. Analysis of the WES Flume Data on Jet Geometry and Dilution	21
	F. Calibration of the Numerical Model of the Jet Regime.	26
	G. Far Field Numerical Model	35
IV.	Design Considerations	40
	A. Diffuser Design Based on Analysis of Inclined Dense Jets in Absence of Ambient Current	40
	B. Analyses of Dense Jets Discharged Upwards Into a Flowing Fluid.	45
	C. Diffuser Design for Desalination Plants	47
V.	Acknowledgments	55
VI.	Bibliography.	56
VII.	Appendices.	58
	A. List of Symbols	58
	B. Characteristic Form for the Far Field Model	61
	C. Comparison of the Numerical Model with the WES Flume Experiments	62

LIST OF TABLES

Table Number		Page
I-I	Properties of Inclined Dense Jets Discharging Into a Still Fluid	4
I-II	Capital and Operating Costs for Diffuser-Outfalls.	5
III-I	Empirical Non-Dimensional Geometry Parameters at the Peak of the Jet Axis .	23
III-II	Values of the Lateral Scale Parameter b, as Deduced from WES Tests	24
III-III	Optimum Values of α and λ for Various Combinations of F_D and F_0 as Evaluated by the Search Routine.	28
III-IV	Coefficients for 3rd Degree Polynomials for α and λ, Equation (36)	30
III-V	Mean Values and Standard Deviations of Pertinent Geometrical and Dilution Parameters	33
IV-I	Jet Geometry and Dilution In Presence of Ambient Current for the 10-MGD Plant . .	49
IV-II	Jet Geometry and Dilution in Presence of An Ambient Current of 0.2 Knots for Different Size Desalination Plants . . .	54
VII-I	Experiments Used for Simulation of the Geometrical Configurations	63

LIST OF FIGURES

Figure Number		Page
III-1	Schematic of Cross-Section for a Neutral Jet in a Cross-Stream	12
III-2	Schematic of Jet Geometry in a Vertical Plane Parallel to the Ambient Flow. . . .	14
III-3	Normalized Plot of Relative Concentration of Effluent Versus r/b within the Jet Regime.	25
III-4	Contours of α Versus F_D and F_e.	31
III-5	Contours of λ Versus F_D and F_e.	32
III-6	Configuration of the 0.2×10^{-4} Concentration Contour at Different x in the Far Field	38
III-7	Field of C at One Cross-Section Far Downstream.	39
IV-1	Densities of Mixed Effluents From Desalination Plants	41
IV-2	Initial Copper Dilution of Effluents From Desalination Plants.	42
IV-3	Design Chart - 10 MGD Plant.	43
IV-4	Dimensions of Jets Injected Upwards into a Flowing Fluid for a 10 MGD Desalination Plant.	50
IV-5	Dilution in Jets Injected Upwards into a Flowing Fluid for a 10 MGD Desalination Plant.	51
IV-6	Diagramatic Representation of Jets into Fluid Flowing at Various Speeds for a 10 MGD Desalination Plant.	52
VII-1	Comparison of Experimental and Model Geometries for Constant F_e and Increasing F_D.	64 64
VII-2	Comparison of Experimental and Model Geometries for Constant F_D and Increasing F_e.	66

List of Figures (continued) Page

VII-3	Comparison of Calculated and Observed Dilutions	69
VII-4	Axial Dilution of Model Plume versus Arc Length Along the Axis for Conditions of Test No. 307	70
VII-5	Axial Dilution of Model Plume versus Arc Length Along the Axis for Conditions of Test No. 309	71
VII-6	Axial Dilution of Model Plume versus Arc Length Along the Axis for Conditions of Test No. 311	72
VII-7	Axial Dilution of Model Plume versus Arc Length Along the Axis for Conditions of Test No. 313	73
VII-8	Axial Dilution of Model Plume versus Arc Length Along the Axis for Conditions of Test No. 304	74
VII-9	Axial Dilution of Model Plume versus Arc Length Along the Axis for Conditions of Test No. 317	75
VII-10	Axial Dilution of Model Plume versus Arc Length Along the Axis for Conditions of Test No. 331	76
VII-11	Axial Dilution of Model Plume versus Arc Length Along the Axis for Conditions of Test No. 345	77

SECTION I. INTRODUCTION

The disposal of effluents from desalination plants has been studied for several years by The Dow Chemical Company under contract to the Office of Saline Water, with Texas A. and M. University as a sub-contractor. Results leading to the model studies of outfalls are reviewed below.

Desalination plants employing variations of the multiple-effect, falling film or multiple-stage, flash distillation processes result in a wastewater stream that is a mixture of brine blowdown and cooling water. Other processes such as reverse osmosis or freezing produce a brine waste stream of a salt concentration depending on the recovery ratio of the process. The chemical composition, and physical properties, of desalination plants effluents and the assessment of the general problems to be encountered in dispersing the wastes and the prediction of the types of marine life likely to be affected by the effluents are detailed in two early OSW Research and Development Reports, (Dow 1967 and 1968). It was concluded that a mixture of brine blowdown and cooling water, under almost all combinations of temperature and salinity, would have a negative bucyancy and would sink to the ocean floor.

At coastal and estuarine locations, an obvious means of disposal of desalination plant effluents is through a properly designed outfall located offshore or at a location in the estuary that minimizes the effects of the combinations of higher salinity, temperature and copper concentration on the bottom organisms.

The proper design of an outfall system is based on the degree of the initial jet dilution of the effluent to meet a predetermined water quality criteria. The mechanism of dilution for the discharge of a single jet into a homogeneous medium of higher density has been the subject of most of the theoretical and experimental studies, (Rawn et.al., 1960, Pearson, 1956, Lawrence, 1962, Fan, 1967, and Hirst, 1971). For design purposes, formulas have been developed to predict with accuracy the initial dilution in a rising jet at the surface of the receiving water (Burchett et.al., 1967), such as encountered where heated water or sewage effluents are disposed into offshore waters.

When the dense effluent from a desalination plant is discharged from one or many ports of a diffuser, it is immediately subjected to a negative buoyancy force proportional to the difference in density between the effluent and the lighter receiving water. The kinetic energy due to the velocity through the port is dissipated in the turbulent mixing of the jet, while the negative bouyancy force drives the effluent toward the floor of the receiving stream, which then moves with the ocean currents or is flushed away by tidal currents in case of an enclosed bay or an estuary.

SECTION I. INTRODUCTION

The experimental study of dense jets, that would be encountered in the disposal of desalination plant effluents, was carried out in laboratory models using still fluid as the receiving environment, by The Dow Chemical Company, Texas Division under contract to the Office of Saline Water. Professor R. O. Reid of Texas A. and M. University as a subcontractor performed the theoretical and numerical analyses of the experimental data.

The preliminary results, (Dow, 1969), established the proportionality of the average height of an upwardly projected dense jet to the flow conditions and density differences and proved the reliability of Turner's Formula (Turner, 1966), under the experimental conditions. An approximate analytical solution of the differential equations governing the flow and density distribution of such a jet was developed. The average height of the jet is given by: (Zeitoun, et.al., 1969),

$$Z_{average} = 0.25 + 0.775 \left[Q_o (E_o g)^{-1/2} \left(\frac{D_o}{2} \right)^{-5/2} \right]$$

The measured distribution of dye concentration across these jets was found to be Gaussian, with two distinctly different slopes identifying a middle region of upward flow, surrounded by an outer region of downward flow. The dilution along the vertical axis of the jet was found to level off to a constant value at a height about two-thirds the ceiling level of the jet. This constant concentration could be explained by a negative entrainment zone, as suggested by Abraham (1967), at which the inner core of the jet is entraining the outer ring of the jet of the same concentration. It was thus concluded that vertical submerged dense jets produce only limited dilution of the effluent due to the negative entrainment resulting from the jet folding on itself.

In the laboratory experimental model, other modes of jet injection studied were: vertical reaching the surface, and inclined at angles of 30°, 45° and 60° from the horizontal, (Dow, 1970). Dense jets having sufficient momentum to reach the surface of the receiving water and spread laterally were found to cover a larger area than comparable completely submerged jets. At the surface the lateral spreading resulted in more dilution of the effluent before the jets started sinking. The surface spreading was found to be oscillatory in nature and mathematically undeterminable. Further quantitative analysis of dense jets reaching the surface was not carried out, since it is not thought to be practial to design a diffuser able to operate in the presence of an ambient current and a sloping ocean floor and to assure that the jets formed would reach the surface.

SECTION I. INTRODUCTION

Nozzels arranged at an angle of 60° from the horizontal produced a maximum effluent trajectory and consequently resultted in the maximum dilution under the same conditions of initial flow.

In the application of the entrainment theory to the inclined dense jets discharging into a still fluid, it was found that the generalized form of the Taylor hypothesis made possible a closer agreement between theory and experiment. This form is given by: (Fox, 1969),

$$q = \left(\alpha - \beta \frac{gEb}{V^2}\right) Vb$$

The best fit to the experimental data was obtained for α = 0.7 and β = -1.0. Both the trajectory data obtained by photographic measurements and the dilution data obtained by dye concentration measurements lead to the same value of α , the entrainment coefficient.

The solutions obtained by numerical computations indicate that the maximum height of inclined jets is proportional to Froude number at the nozzle raised to a power of 1.1.

$$Z_m/D \propto F^{1.1}$$

Linear correlations of the inclined jet dimensions and the dilution found at the top of the jet, as a function of the Froude numbers, are given in Table I-I. The error introduced by a linear correlation as compared to the exponent correlation predicted by theory is negligible in the range of the Froude numbers used in the design of diffuser systems.

Diffuser design charts were developed for desalination plants procueding 2, 5, 10, and 50 million gallons per day of fresh water. These charts are plots of the maximum height of a 60° angle jet versus Froude number at the diffuser ports for different port diameters and initial velocities through the ports. The number of ports for each choice of variables and the flow rate of effluent from a desalination plant is indicated on the chart and is related to the degree of dilution required.

Conceptual designs were made for the four desalination plants. The outfall pipelines and diffusers were designed to convey the effluent from a point 800 feet inland to a point outside the violent surf zone. Sizes and types of pipe were selected for maximum economy considering initial capital cost, method of construction, operating and maintenance costs, and the corrosive nature of the marine environment. Gravity flow, rather than pumped

SECTION I. INTRODUCTION

TABLE I-I

PROPERTIES OF INCLINED DENSE JETS DISCHARGING INTO A STILL FLUID

Initial Angle of Jet	Z_m/D	X_m/D	$S_o=C_o/C$
60°	2.04 (F)	3.28 (F)	F/1.8
45°	1.43 (F)	3.33 (F)	F/2.4
30°	1.15 (F)	3.48 (F)	F/2.8

Z_m = Maximum height of the top boundary

X_m = Maximum horizontal spread of jet

F = Froude Number = $\dfrac{V_o}{\sqrt{E_o g D}}$

$E_o = \dfrac{\rho_o - \rho_e}{\rho_e}$, U_o = velocity through nozzle

D = Diameter of nozzle

S_o = Dilution at the top of the jet

TABLE I-II

CAPITAL AND OPERATING COSTS FOR DIFFUSER-OUTFALLS (1)

PLANT SIZE (MGD)	CONSTRUCTION COST ($)	ANNUAL OPERATING COSTS ($)	COST/1000 GL (¢)
2	730,000	60,080	9.1
5	766,000	62,630	3.8
10	857,000	69,550	2.1
50	1,320,000	108,870	0.66

(1) Dow, 1970

flow was recommended for all systems. Steel pipe was selected for the 2-, 5-, and 10- MGD plants, and prestressed concrete pipe was selected for the 50-MGD plant. A summary of the cost estimate for the four different sizes of desalination plants is given in Table I-II.

The developed conceptual designs (Dow, 1970) are based on the degree of initial jet dilution of a dense effluent injected at a 60° angle in a still receiving fluid. Although this situation does not exist in actual streams, it is thought to represent a limiting worst condition, and therefore the presence of currents would increase the dilution over the design value. This criteria needed to be verified in a system where ocean currents or tidal currents could be applied. Such facilities were available at the United States Army Engineer Waterways Experiment Station at Vicksburg, Mississippi.

A joint effort between The Dow Chemical Company, Texas A. and M. University and the Waterways Experiment Station was arranged by the Office of Saline Water for the conduction of model studies and the analyses of the results.

The proposed tasks under the contractual arrangement for The Dow Chemical Company and Texas A. and M. University were:

A. Assist in the design of the experiments to be carried on in the flume model and in the model bays at Vicksburg in order to approach realistic modeling of expected outfall conditions.

B. Coordinate the data reduction and assist in the interpretation of the obtained mixing data to determine whether any modifications to the conceptual outfall designs being tested will be desirable or economically justifiable.

C. Program and carry on a series of numerical experiments to cover a wide range of Froude numbers, and ambient current speeds to evaluate the dispersal of effluent under the influence of currents past the source.

D. Develop alternate designs for outfalls for smaller desalting operations for which the previously developed conceptual designs are not readily economically suitable.

Experiments at the U. S. Army Engineer Waterways Experiment Station were conducted in two areas:

1. Tests of single- and multiple-port diffusers at an undistorted scale of 1:20 in a flume having a level bottom and conveying uniform steady flow. Results have been published as Part I of this report "Flume Study of the Mixing Characteristics of Dense Jets Discharged Into a Flowing Fluid". (U. S. Army, 1971)

2. Tests of multiple-port diffusers in three distorted estuary models. These models were of San Diego Bay, Galveston Bay, and Delaware River. The objectives of these tests were to determine dispersion rates of the brine waste and to define the dynamic equilibrium distribution of the waste after the plant being simulated had been in operation for some time. The results of these tests have been published as Part II of this report, "Tests of Effluent Dispersion in Selected Estuary Models." (U. S. Army, 1971)

The coordination of the work conducted by the three parties was achieved during several meetings at the Waterways Experiment Station at Vicksburg. The results of the flume model experiments, that is concerned with the initial mixing of the dense effluents with the receiving water in the near field, and could affect the design of the diffusers, were used in the numerical simulation studies. This part of the report presents the numerical simulation and the design considerations resulting from the modeling of diffusers in presence of an ambient current.

SECTION II. SUMMARY AND CONCLUSIONS

Although at coastal locations, the saline dense effluent from a desalination plant is potentially harmful to the marine organisms, the environmental effects can be minimized or eliminated if the effluent is properly mixed with and diluted by the receiving water.

Conceptual designs of outfall diffuser systems were previously developed (Dow, 1970) on the basis of laboratory tests of the initial jet dilution of a dense effluent injected at a 60° angle in a still receiving fluid.

The experimental verification of the conceptual designs in the presence of an ambient current by the United States Army Corps of Engineers were published as Parts I and II of this report: "Flume Study of the Mixing Characteristics of Dense Jets Discharged Into a Flowing Fluid", and "Tests of Effluent Dispersion in Selected Estuary Models", respectively.

The data obtained in the flume study were used to calibrate several pertinent existing models for the jet regime. The model chosen gives a reasonable simulation of the geometry of the jet axis and of the dilution at the peak of the jet, but was found to overestimate the lateral spreading factor. A far-field plume model was also developed and applied to the prediction of the plume size and the dilution downstream from the diffuser.

A summary of the correlations developed to estimate the jet geometry and dilution in the presence of an ambient current is given below:

Maximum height of upper boundary of Jet:	$Z_m = 3.4 \times 10^{-0.148 F_e} (D_o F_D)$
Distance downstream where Jet falls to bottom:	$X_o = 9.62 Z_m \log (2 F_e)$
Lateral Spread at X_o:	$W_o = 1.51 Z_m \log (4.91 F_e)$
Dilution at the axis of the Jet at its peak:	$S = 18 e^{0.8 F_e}$
Minimum Dilution in the Plume:	$\varepsilon_m = 31 \times 10^{0.4 F_e} \left(\frac{X}{X_o}\right)^{0.68}$

The definitions of the terms are given in the Appendix.

SECTION II. SUMMARY AND CONCLUSIONS

The application of these equations to the design of diffusers required by variously sized desalination plants and in the presence of various ambient currents is outlined in Section IV. The dilutions obtained in the presence of currents as low as 0.1 knots were found to be higher than those calculated for a 60° angled jet in a still fluid.

It is concluded that, the design concepts developed for a still receiving fluid represent a limiting worst condition, and that the presence of currents increases the dilution over the design value.

It is thus recommended that the conceptual design methods previously developed for a still receiving fluid, be used to represent that limiting condition. For more accurate prediction of the plume size and actual dilutions under known ambient conditions the equations presented in this report are more satisfactory.

The cost of the diffuser is a small part of the total cost of an outfall system designed to convey the effluent to a point outside the violent surf zone. For small size desalination plants, less than 5 MGD, the dispersion of the effluents near the shore inside the surf zone seems to be the only way to eliminate the high cost of the near shore section of the outfall system. The removal of copper from the effluent before it is dispersed into the surf zone may be found to be necessary if the flushing of the effluent is inhibited by the geomorphology of the location.

SECTION III. NUMERICAL SIMULATION OF THE DISPERSION OF A DENSE EFFLUENT DISCHARGE INTO A HOMOGENEOUS STREAM (Texas A. and M. University)

A. Introduction

Our efforts during the past year have been to explore various theoretical models of dense jets discharged vertically into a homogeneous steady stream in the attempt to simulate the flume experiments concerning the same problem which have been carried out at the Waterways Experiment Station (WES). The latter experiments include measurements of jet geometry and of dilution for a wide range of densimetric Froude number and ratio of port velocity to ambient stream velocity. Most of the tests were carried out for a single circular port. The analysis reported here is confined to this situation. Moreover it is assumed that the ambient fluid is uniform in density and uniform in horizontal speed.

One can distinguish essentially two different regimes of the dense effluent based upon geometry and character of the flow within the effluent. The first is the jet regime in which the axial velocity of the effluent significantly exceeds that of the ambient fluid and in which a similarity of axial velocity and effluent distribution exists at all sections transverse to the jet axis. Essentially this regime is confined to the region upstream of the point where the arcing axis of the jet strikes the flume base. Throughout this regime the influence of gravity on the dense effluent is to produce a downward acceleration of the fluid, thus placing a limit (assuming the fluid is sifficiently deep) on the maximum height of the initially vertically directed jet.

Downstream from the point of contact of the axis of the jet with the flume bed, the effluent is no longer being accelerated downwards as a body, however, the combination of gravity and the distribution of effluent produce a transverse pressure gradient which enhances the transverse horizontal spreading of the effluent (in the form of an internal gravity wave). Moreover in this regime the axial velocity tends to be nearly that of the ambient stream. We will refer to this regime as the far field plume in contrast with the near field arcing jet.

Most previous experimental studies of jets discharged into a stream have been confined to either neutral jets or positively buoyant jets. The WES data accordingly represents a unique set in that it is confined to negatively buoyant conditions. One might expect that the negatively buoyant (or dense case) is simply an inverted version of the positively buoyant case. This may be nearly true for an ambient fluid

which is nominally at rest. However for a moving fluid there is an important qualitative difference in the jet regime which influences the degree of entrainment for the positive versus the negative buoyancy cases.

It is well known that for a neutral jet discharged into a cross-stream the influence of the ambient flow is to produce vortices as shown schematically in Figure III-1. Moreover, the concentration and axial velocity distribution is distorted from circular form to a kidney shape (Abramovich 1963). This internal circulation tends to enhance the entrainment process.

On the other hand for a dense jet whose axis is parallel to the ambient flow (i.e., near the peak of an arcing jet) the action of gravity and non-uniform density produces a transverse circulation pattern just opposite to that shown in Figure III-1 (see for example Csanady, 1965 or Crew, 1970). The reverse would be true for a positively buoyant jet. Thus the density-induced circulation in a dense plume tends to cancel out the cross-stream induced circulation, while it is enhanced in the case of the buoyant plume. The fact that the WES dilution data shows nearly circular contours in the jet regime beyond the peak height is indirect evidence of this. In view of these qualitative differences in the physics, it is not surprising that the final similarity model chosen in the present study of the jet regime differes from all of the existing models. The latter seem to work only for neutral or buoyant jets.

The main effort has been in connection with the simulation of the WES geometry and dilution data in the jet regime. The Crew (1970) model can in principle be applied to the far field plume regime, however it does involve considerable computer time. An alternative approximate scheme which still allows for internal gravity wave phenomena but is more economical in respect to computer time is suggested here, but real time limitations have not allowed an adequate comparison of this scheme with the WES data.

The presentation which follows includes: a comparison of pertinent existing models for the jet regime; the model chosen for this study; the non-dimensional working form for the model; an analysis of the WES geometry data and of the dilution data in form suitable for calibration of the chosen model; calibration of the jet regime model; predictions of the model compared with data not used in the calibration; and finally a discussion of a far field plume model with an illustration of its application.

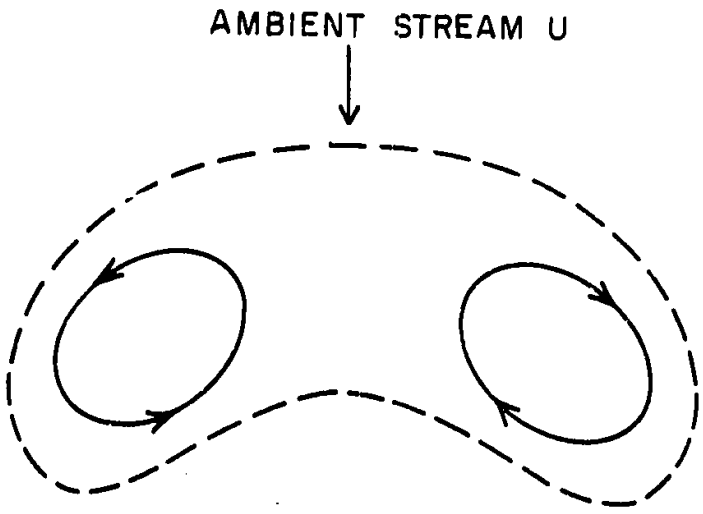

Figure III-1

Schematic of cross-section for a neutral jet in a cross-stream. Full lines are streamlines. Dashed curve is a contour of effluent concentration.

SECTION III. NUMERICAL SIMULATION OF THE DISPERSION OF A DENSE EFFLUENT DISCHARGE INTO A HOMOGENEOUS STREAM (Texas A. and M. University)

B. Comparison of Some Existing Models for the Jet Regime in a Cross-Stream

We will confine attention to effluent which is discharged vertically into a uniform stream so that the jet axis is a curve in a vertical plane parallel to the ambient stream. We will take the coordinate x downstream and z vertically upwards, the orgigin being taken at the nozzle opening, which in general is at a displacement D above the floor of the flume (Figure III-2). In the case of the WES tests D is the supply pipe diameter, while D_o is the diameter of the vertically directed port. The angle between the axial velocity of the jet and the horizontal for some point P on the jet axis is designated θ (Figure III-2). The ambient current is U.

All of the axially symmetric similarity models for jets assume that the concentration of effluent, say C, has the form

$$C = E\, f(r/b)$$

where E and b are functions of arc length s from the orifice and r is radial distance from the axis of the jet. If $f(0) = 1$ then E represents the axial value of concentration C. The quantity b is a lateral scale parameter. In the case of the so-called "top hat" profile, b is the outer boundary of the concentration. In the case of a Gaussian distribution we will regard b as the standard deviation (i.e., for the Gaussian case $f(r/b) = \exp(-r^2/2b^2)$).

The departure of the jet velocity from the local parallel component of ambient velocity ($U \cos\theta$) is also assumed to be of a form similar to that for C.

Under these conditions one can obtain laterally integrated versions of the equations of conservation of mass and momentum of the form (see for example Hirst, 1971, which contains a very thorough analysis).

$$\frac{d}{ds}(Vb^2) = q_e, \qquad (1)$$

$$\frac{d}{ds}(Vb^2E) = 0, \qquad (2)$$

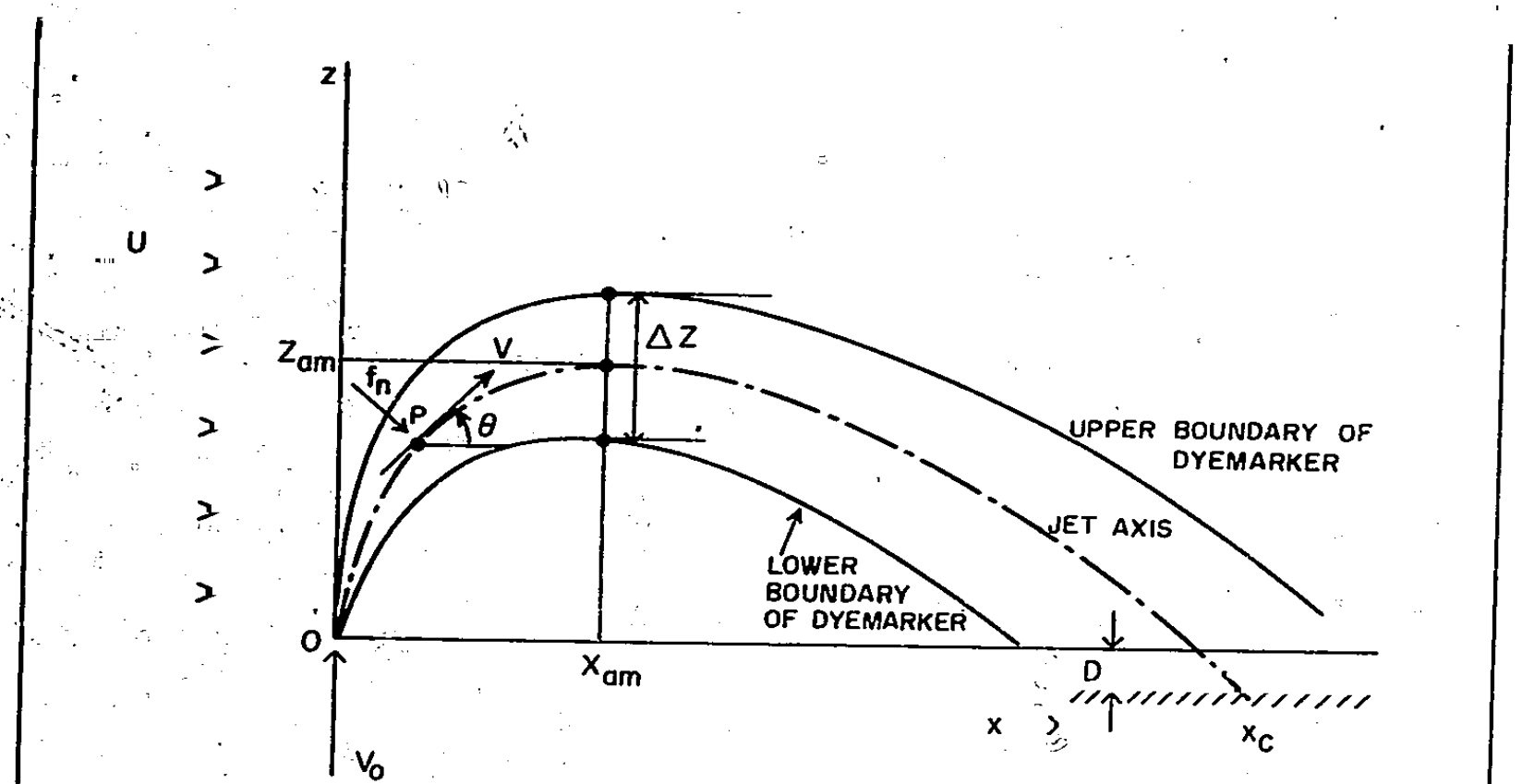

Figure III-2

Schematic of jet geometry in a vertical plane parallel to the ambient flow.

SECTION III. NUMERICAL SIMULATION OF THE DISPERSION OF A DENSE EFFLUENT DISCHARGE INTO A HOMOGENEOUS STREAM (Texas A. and M. University)

$$\frac{d}{ds}(V^2b^2) = q_eU\cos\theta - \lambda gEb^2\sin\theta, \tag{3}$$

$$\frac{d\theta}{ds} = \frac{-f_n - \lambda gEb^2\cos\theta}{(Vb)^2} \tag{4}$$

where V is an effective axial conveyance velocity, q_e is the volume of entrainment per unit arc length per unit time, g is gravity, λ is a non-dimensional coefficient which theoretically depends upon the form of the distrubtion profile f(r/b), and f_n is an effective lateral force per unit length acting normal to the axis of the jet (see Figure III-2). For a non-neutral jet

$$E = \frac{\rho_m - \rho_e}{\rho_e} \tag{5}$$

where ρ_m is the local density at the axis of the jet and ρ_e is the environmental density. For the dense jet $E > 0$.

Essentially all of the existing similarity models in the literature are of the form (1) to (4), provided that the velocity and concentration have the same scale parameter b. If one allows for a different lateral scale for velocity and concentration then the effective conveyance velocity for E in (2) is slightly different from V (see for example Hirst, 1971).

The main difference among the various models concerns the form of the entrainment flux q_e, the form of the normal thrust f_n and the value chosen for λ. Before discussing the particular forms for q_e and f_n, it is pertinent to point out a general property of the above set of equations for the case of a neutral jet. In this case, an initially vertical jet will bend over due to f_n and tend to approach the horizontal. Thus, at sufficient distance, $d(V^2b^2)/ds$ tends to approach q_eU. If we combine this with (1) we find that $Vb^2(V-U)$ approaches a constant; moreover since Vb^2 tends to grow without limit we see that V will approach U, as must ultimately be the case in the far field. Indeed any other form for the entrainment term for momentum in (3) relative to the volume entrainment term in (1) would be untenable.

SECTION III. NUMERICAL SIMULATION OF THE DISPERSION OF A DENSE EFFLUENT DISCHARGE INTO A HOMOGENEOUS STREAM (Texas A. and M. University)

With regard to the specific form for f_n there are essentially two which have been employed in previous studies. The first form is based on the concept of form drag as occurs for flow normal to a rigid cylinder, namely

$$f_n = C_d b U^2 |\sin\theta| \sin\theta. \tag{6}$$

where C_d is an appropriate drag coefficient which must be evaluated empirically. Note that the sign of f_n depends upon the sign of θ. Thus it can be negative after the jet reaches its peak and is in the descent stage. This property is also true of the alternate form (7).

The second form for f_n treats this effective trust per unit length as a rate of entrainment of lateral momentum. In this case

$$f_n = \gamma\, q_e U \sin\theta, \tag{7}$$

where γ is a non-dimensional constant.

The model of Fan (1967) employs the drag force form (6). Also the experimental relations obtained by Keffer and Baines (1963) for a neutral jet yield a curvature consistent with (6).

On the other hand, the analysis of Pratte and Baines (1967) and that of Hirst (1971) imply and/or make use of the form (7).

In regard to relations for the entrainment rate, q_e, the following forms have been employed:

Morton (1961)

$$q_e = \alpha |V - U| b \; ; \tag{8}$$

Keffer and Baines (1963)

$$q_e = \alpha (V - U) b \; : \tag{9}$$

Fan (1967)

$$q_e = \alpha^b \left[(U \sin\theta)^2 + (V - 2U\cos\theta)^2 \right]^{1/2} \; ; \tag{10}$$

SECTION III. NUMERICAL SIMULATION OF THE DISPERSION OF A DENSE EFFLUENT DISCHARGE INTO A HOMOGENEOUS STREAM (Texas A. and M. University)

Hirst (1971)

$$q_e = (\alpha_1 - \alpha_2 \frac{gEb}{V^2} \sin\theta) \left| V - U\cos\theta \right| b + \alpha_3 Ub. \qquad (11)$$

In the first three of these relations the coefficient α is not necessarily the same (nor is the same notation employed in the cited paper). The more complicated form given by Hirst includes a generalization of the type first suggested by Fox (1970) in which the local Froude number $V/(gEb)^{1/2}$ enters, as in the first term on the right of (11). The second term in effect allows for turbulence within the ambient fluid.

It is noteworthy that Keffer and Baines (1963) as well as Fan (1967) found that in order to fit the available data, α must be an increasing function of U/V_o where V_o is the port velocity of the jet. In addition, Keffer and Baines found that α must increase with S/D_o if (9) is to be consistent with the data which they analyzed (neutral jets only).

It is also pertinent to note that the relations of Morton (1961), Fan (1967) and Hirst (1971) assert that q_e can be positive even if V falls below U cos θ. In fact, the Hirst relation asserts that $q_e > 0$ when $V = U\cos\theta$.

In regard to the coefficient λ in (3) and (4), the following values have been employed:

Morton (1961)

$$\lambda = 1$$

Fan (1967) and Hirst (1971)

$$\lambda = 2.$$

These values are based upon "top hat" and Gaussian distributions, repsectively.

Hirst (1971) used $\lambda = 2$ for the case where b is the same for velocity and concentration.

SECTION III. NUMERICAL SIMULATION OF THE DISPERSION OF A DENSE EFFLUENT DISCHARGE INTO A HOMOGENEOUS STREAM (Texas A. and M. University)

C. Model Chosen for the Present Study of the Dense Jet Regim

About five different models were experimented with in the attempt to simulate the WES flume data. These included the Fan (1967) model, a model similar to Fan's but allowing for different lateral scales for density and velocity distribution, and two models very similar to that of Hirst (1971). None of these were satisfactory for both geometry and dilution data.

The final model chosen makes use of (1) through (4) with

$$q_e = \alpha V b \tag{12}$$

and

$$f_n = C_d U^2 b \left|\sin \theta\right| \sin \theta. \tag{13}$$

The relation (12) allows for entrainment even if V falls to the value U cos θ, just as does the Hirst relation (11). The main distinction between the chosen model and those of Fan, Hirst and others is that both α and λ are allowed to be functions of the port densimetric Froude number and a Froude number based on the ambient flow. To be specific, we define these two Froude numbers as follows:

$$F_D = \frac{V_o}{(gE_oD_o)^{1/2}}, \tag{14}$$

$$F_e = \frac{U}{(gE_oD_o)^{1/2}}, \tag{15}$$

where V_o is the jet velocity at the port, which is of diameter D_o, and $E_o = (\rho_o - \rho_e)/\rho_e$, ρ_o being the initial density of the effluent at the port. Note that F_e is simply U/V_o times F_D. The F_D used here is the same as that employed in the WES analysis.

Thus in the present model we consider:

$$\alpha = \alpha(F_D, F_e)$$

$$\lambda = \lambda(F_D, F_e). \tag{16}$$

The functional form is determined empirically by fitting the predictions of the model at the position X_{am} (see Figure III-2) to the data for this position. This fitting process will be described in later sections.

In order to complete the specification of the numerical model, we must add to relations (1) to (4) the following equations appropriate to the jet geometry:

$$\frac{dx}{ds} = \cos\theta$$

$$\frac{dz}{ds} = \sin\theta. \tag{17}$$

In addition we take as boundary conditions at s = o:

$$b = D_o/2$$

$$V = V_o$$

$$E = E_o \tag{18}$$

$$\theta = 90^o ,$$

where D_o, V_o and E_o are as previously defined.

D. Non-Dimensional Form of the Model

It is convenient in the numerical integration to convert the differential equations of the model to non-dimensional form. We define a non-dimensional volume flux and momentum flux as follows:

$$M \equiv Vb^2/V_o b^2_o , \tag{19}$$

$$J \equiv (Vb)^2/(V_o b_o)^2 , \tag{20}$$

where $b_o = D_o/2$. Moreover let

$$\xi = x/D_o$$
$$\eta = z/D_o \qquad (21)$$
$$\zeta = s/D_o \ .$$

Eqs. (1), (3), (4) and (17) are then converted to

$$\frac{dM}{d\zeta} = 2\alpha J^{1/2} \qquad (22)$$

$$\frac{dJ}{d\zeta} = 2\alpha \frac{F_e}{F_D} J^{1/2} \cos\theta - \frac{\lambda}{F_D^2} \frac{M}{J} \sin\theta \qquad (23)$$

$$J \frac{d\theta}{d\zeta} = -2 C_d \left(\frac{F_e}{F_D}\right)^2 \frac{M}{J^{1/2}} \left|\sin\theta\right| \sin\theta - (\lambda/F_D^2)(M/J)\cos\theta \qquad (24)$$

$$\frac{d\xi}{d\zeta} = \cos\theta \qquad (25)$$

$$\frac{d\eta}{d\zeta} = \sin\theta \ . \qquad (26)$$

Eq. (2) with the boundary conditions takes the form

$$\frac{E_o}{E} = M, \qquad (27)$$

which is a measure of the dilution relative to the source. Moreover from definitions (19) and (20) we get

$$\frac{b}{b_o} = \frac{M}{J^{1/2}} \qquad (28)$$

$$\frac{V}{V_o} = \frac{J}{M} \ .$$

The boundary conditions are as follows:

$$\left.\begin{aligned} M = J &= 1 \\ \xi = \eta &= o \\ \theta &= 90^o \end{aligned}\right\} \quad \text{at } \zeta = o \tag{29}$$

Numerical integration of (22) through (26) was carried out using a Runge-Kutta scheme with uniform increments of ζ. In the initial work $\Delta\zeta$ was taken as 0.10; however, it was found that an increment of 1.00 yielded nearly comparable accuracy and afforded a considerable saving of machine time.

E. Analysis of the WES Flume Data on Jet Geometry and Dilution

As remarked earlier the calibration of the model (i.e., the evaluation of α and λ vs. F_D and F_e) was carried out by fitting the model to the WES data appropriate to the peak position of the axis of the jet (i.e., at $x = X_{am}$; Figure III-2).

Values of X_{am}, Z_{am}, ΔZ (Figure III-2) were read from the estimated axis for the jet profiles given in the Appendices C and D of Part I of the WES report. Z_{am} is adjusted so as to represent height above the port rather than the flume floor. A total of 309 sets of such values were obtained; this includes 115 sets from the 115 tests for the 3 inch port, 149 sets out of the 166 tests for the 6 inch port and 45 sets out of the 80 tests for the 9 inch port. From these sets of data, the following non-dimensional quantities were computed:

$$X_m^* = \frac{X_{am}}{D_o\, F_D\, F_e^{\,1/2}} \tag{30}$$

$$Z_m^* = \frac{Z_{am}}{D_o\, F_D} \times 10^{0.148 F_e} \tag{31}$$

$$\Delta Z^* = \frac{\Delta Z}{Z_{am}} \tag{32}$$

Relation (31) is based on the empirical equation for the maximum height for the upper boundary given in the WES report, Part I. For the axis we expect a similar relation but with a smaller constant of proportionality (Z_m^*).

SECTION III. NUMERICAL SIMULATION OF THE DISPERSION OF A DENSE EFFLUENT DISCHARGE INTO A HOMOGENEOUS STREAM (Texas A. and M. University)

Each of the quantities X_m^*, Z_m^*, ΔZ^* varies randomly from test to test about a mean value, there being no apparent systematic variation of these quantities with F_D or F_e. The mean values and standard deviations of each of the above quantities are listed in Table III-I. This shows a reasonable consistency among the tests for the three separate port sizes.

The values of dilution as measured on the jet axis in the WES flume tests were grouped according to F_e and F_D and interpolated for the position X_{am} on the axis. These dilution values are denoted by S. It was found that the following empirical relation fit this dilution data quite well:

$$S = 18\, e^{0.80F_e} , \tag{33}$$

independent of F_D.

Also from the dilution data within the jet regime where the dilution contours in a plane normal to the axis are reasonably circular, values of the scale factor b were estimated by fitting a Gaussian relation to the contour data. This was done as follows. The area (A) enclosed by a given dilution contour (ϵ) was evaluated by planimeter and properly scaled to prototype conditions. The equivalent radius r for a true circular contour was evaluated from the relation $\pi r^2 = A$. A plot of log ϵ versus r^2, including the axial value ϵ_{min} at $r = 0$, was constructed for each cross-section for which dilution measurements were made in the jet regime. From the slope of the straight line of best fit, the value of b^2 could be estimated corresponding to the relation

$$\frac{\epsilon_{min}}{\epsilon} = e^{-r^2/2b^2} .$$

The resulting values of b along with other pertinent quantities are shown in Table III-II.

A normalized composite plot of relative concentration versus r/b based upon the WES dilution data for the jet regime is presented in Figure III-3. This shows that the lateral distribution is very nearly Gaussian, the deviations being essentially random.

SECTION III. NUMERICAL SIMULATION OF THE DISPERSION OF A DENSE EFFLUENT DISCHARGE INTO A HOMOGENEOUS STREAM (Texas A. and M. University)

TABLE III-I

EMPIRICAL NON-DIMENSIONAL GEOMETRY PARAMETERS AT THE PEAK OF THE JET AXIS

D_o	n		X_m^*	Z_m^*	ΔZ^*
3"	115	mean	1.720	2.233	0.914
		Std. Dev.	0.753	0.511	0.412
6"	149	mean	1.729	2.287	0.950
		Std. Dev.	0.653	0.426	0.282
9"	45	mean	2.091	2.511	0.853
		Std. Dev.	0.783	0.332	0.142
Overall	309	mean	1.778	2.300	0.922
		Std. Dev.	0.723	0.457	0.325

SECTION III. NUMERICAL SIMULATION OF THE DISPERSION OF A DENSE EFFLUENT DISCHARGE INTO A HOMOGENEOUS STREAM (Texas A. and M. University)

TABLE III-II

VALUES OF THE LATERAL SCALE PARAMETER b AS DEDUCED FROM WES TESTS

Test	F_D	F_e	X (ft.)	Min. Dil.	b (ft.)
420	36.3	2.055	40	262	3.75
420	36.3	2.055	80	489	3.08
615	13.1	0.291	5	40	3.88
619	25.0	0.291	10	36	6.08
619	25.0	0.291	20	49	6.16
623	13.2	0.581	10	64	3.25
625	18.3	0.581	20	42	5.22
627	25.1	0.581	20	21	5.44
627	25.1	0.581	40	44	6.32
629	32.6	0.581	20	20	5.66
629	32.6	0.581	60	41	12.48
633	19.0	0.872	40	56	6.50
635	25.2	0.872	40	66	7.05
637	32.9	0.872	40	77	4.33
643	24.7	1.279	40	40	5.09
645	32.7	1.279	40	44	5.06
645	32 7	1.279	100	75	11.13
655	13.3	1.453	40	80	3.67
657	18.7	1.453	40	71	5.37
659	24.6	1.453	40	85	5.51
659	24.6	1.453	80	172	11.44
661	32.1	1.453	40	64	5.77
661	32.1	1.453	80	115	10.70
665	18.6	2.180	40	125	3.98
665	18.6	2.180	80	240	6.87
667	24.2	2.180	40	128	4.78
667	24.2	2.180	80	143	5.73
669	31.7	2.180	40	95	5.02
669	31.7	2.180	80	178	6.92
669	31.7	2.180	160	218	7.54
673	18.3	2.906	40	250	4.26
673	18.3	2.906	80	365	5.91
675	24.6	2.906	40	237	5.43
675	24.6	2.906	80	382	6.40
677	32.1	2.906	40	178	4.80
677	32.1	2.906	80	363	6.88
677	32.1	2.906	160	700	11.57
694	26.8	2.008	40	105	4.37
694	26.8	2.008	80	238	7.13

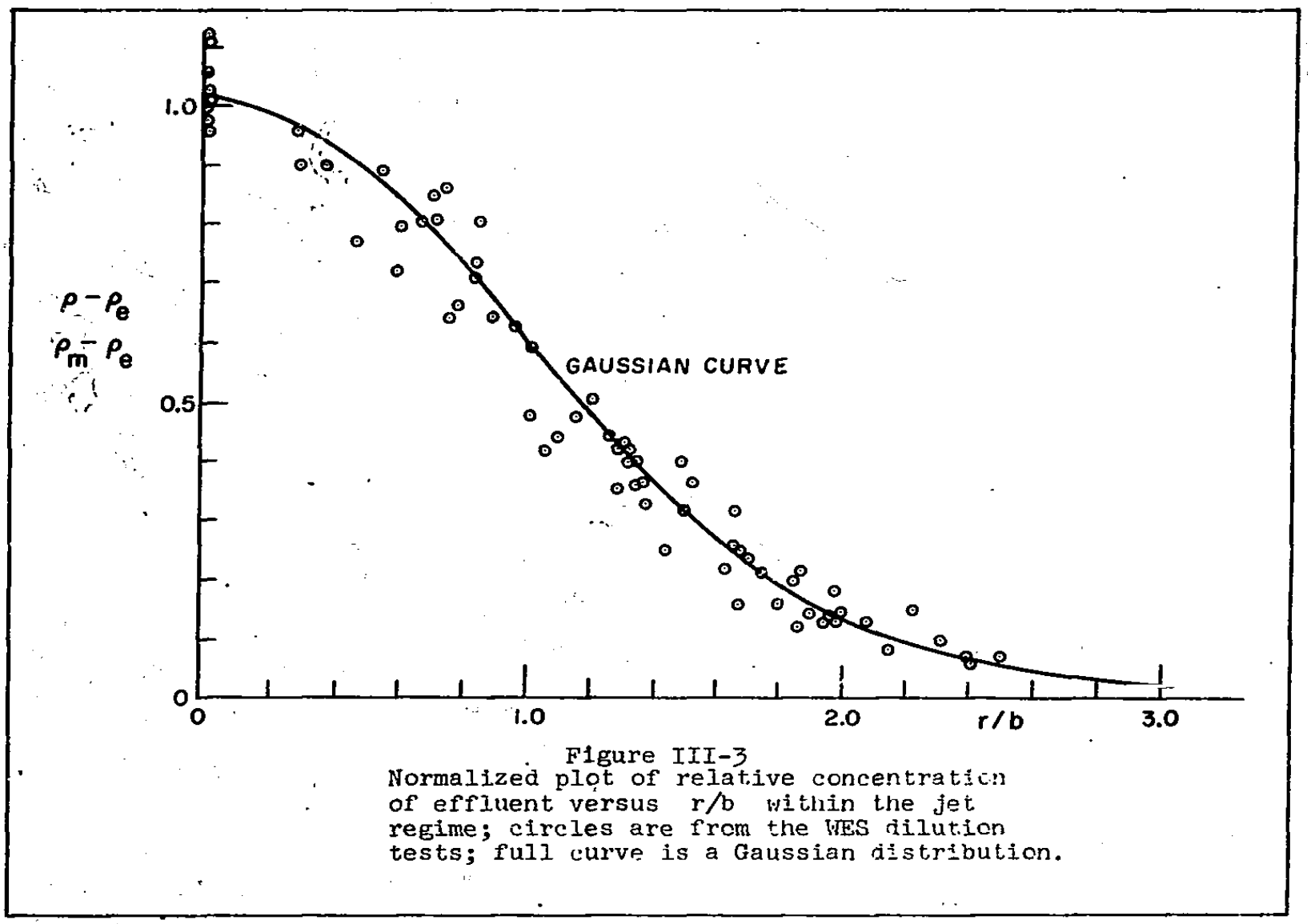

Figure III-3
Normalized plot of relative concentration of effluent versus r/b within the jet regime; circles are from the WES dilution tests; full curve is a Gaussian distribution.

SECTION III. NUMERICAL SIMULATION OF THE DISPERSION OF A DENSE EFFLUENT DISCHARGE INTO A HOMOGENEOUS STREAM (Texas A. and M. University)

F. Calibration of the Numerical Model for the Jet Regime

The bulk of the calculations were carried out for 49 pairs of F_D, F_e values (see Eqs. (14) and (15)) which were selected as representative of the ranges of these variables in the WES tests. Specifically seven values of each were chosen as follows:

$$F_D = 13.0,\ 18.0,\ 22.0,\ 26.0,\ 32.0,\ 38.0,\ 52.0$$

$$F_e = 0.40,\ 0.80,\ 1.30,\ 1.70,\ 2.30,\ 3.00,\ 4.00$$

These yield a total of 49 possible combinations each of which represents about the same frequency of occurrence with respect to the WES flume tests.

For a given F_D, F_e and with a given set of coefficients α, λ, C_d, Eqs. (22), (23), (24), (25) and (26) were integrated numerically from the port up to the peak position of the jet axis (where $\theta = 0$) yielding values of E_o/E, b/b_o, V/V_o, ξ, η at this position. From these the quantities X_m^*, Z_m^* as defined by (30) and (31) were computed. In addition b_m/Z_{am}, V/U and a normalized dilution, S^*, were evaluated again for the peak position on the jet. The quantity S^* is defined by

$$S^* = \frac{E_o/E}{S} \tag{34}$$

where S is given by (33). If the numerical model simulates the experimental data, then X_m^* should be 1.778, Z_m^* should be 2.300, S^* should be 1.000 and b_m/Z_{am} should be a constant (its value being unknown).

From preliminary test calculations it was found that the results were not too sensitive to variations of C_d compared with variations of α and λ. Accordingly C_d was held fixed at a value of unity.

In order to find the optimum combination of α and λ for given F_D and F_e a special program was constructed to search for that combination of α and λ which minimizes the error function.

$$e_r = w_1 (X_m^* - 1.778)^2 + w_2 (Z_m^* - 2.300)^2 + w_3 (S^* - 1.000)^2, \tag{35}$$

where w_1, w_2, w_3 are positive weighting parameters. These were taken as 1, 1, 3, respectively, thus placing more importance on proper simulation of the dilution data.

The search program starts with an assigned pair of α,λ in the range 0 to 2 and, with the appropriate logic routine, marches along that path in the α, λ diagram (at uniform increments of α,λ) which leads it towards a minimum value of e_r. Once the minimum is found, based on the initial choice of $\Delta\alpha$, $\Delta\lambda$, then the latter intervals are halved and the search is continued with finer resolution. This is repeated until the optimum α,λ for given F_D, F_e are within 0.0125 of the true values for each.

At each step in the search operation, a numerical integration of the type discussed above is carried out. Moreover, 49 such search operations were carried out corresponding to the 49 selected pairs of test parameter F_D, F_e.

The resulting optimum α,λ for given F_D, F_e are given in Table III-III along with their error parameter e_r. Where no values are given for e_r, the program failed to converge to an optimum because the jet maximum was not reached in a reasonable number of integration steps. Values of α,λ which are in parentheses are interpolated with respect to F_D.

In order to expedite further computation, it is convenient to approximate the optimum α and λ versus F_D and F_e by polynomial relations of appropriate degree (n):

$$\alpha = \sum_{j+k=0}^{n} A_{jk} F_d^j F_e^k$$

$$\lambda = \sum_{j+k=0}^{n} B_{jk} F_d^j F_e^k \qquad (36)$$

The coefficients based upon third degree polynomials are given in Table III-IV. Contours of α and λ, based upon the fitted relations, are shown respectively in Figures III-4 and III-5.

SECTION III. NUMERICAL SIMULATION OF THE DISPERSION OF A DENSE EFFLUENT DISCHARGE INTO A HOMOGENEOUS STREAM (Texas A. and M. University)

TABLE III-III

OPTIMUM VALUES OF α AND λ FOR VARIOUS COMBINATIONS OF F_D AND F_e AS EVALUATED BY THE SEARCH ROUTINE

(The error function e_r is defined by (35))

F_D	F_e	α	λ	e_r
13.0	0.4	0.4000	0.2500	0.0171
13.0	0.8	0.4000	0.3750	0.1323
13.0	1.3	0.4250	0.5625	0.3445
13.0	1.7	0.4250	0.7375	0.4336
13.0	2.3	0.4250	1.0500	0.5088
13.0	3.0	0.4250	1.4500	0.6188
13.0	4.0	0.3255	1.4125	1.5411
18.0	0.4	0.3000	0.3000	0.1342
18.0	0.8	0.3125	0.4000	0.0258
18.0	1.3	0.3375	0.5375	0.1651
18.0	1.7	0.3625	0.6875	0.2441
18.0	2.3	0.3625	0.9250	0.3035
18.0	3.0	0.3625	1.2875	0.3993
18.0	4.0	(0.3089)	(1.3993)	---
22.0	0.4	0.2625	0.3375	0.2758
22.0	0.8	0.2625	0.4125	0.0074
22.0	1.3	0.2875	0.5250	0.0850
22.0	1.7	0.3125	0.6500	0.1482
22.0	2.3	0.3125	0.8375	0.2286
22.0	3.0	0.3125	1.1125	0.3838
22.0	4.0	(0.2957)	(1.3885)	---
26.0	0.4	0.2125	0.3750	0.4186
26.0	0.8	0.2375	0.4500	0.0084
26.0	1.3	0.2625	0.5375	0.0370
26.0	1.7	0.2875	0.6375	0.0882
26.0	2.3	0.3000	0.8375	0.1369
26.0	3.0	0.3000	1.0875	0.2657
26.0	4.0	(0.2824)	(1.3783)	---
32.0	0.4	0.1875	0.4250	0.6365
32.0	0.8	0.2125	0.4875	0.0537
32.0	1.3	0.2375	0.5625	0.0074
32.0	1.7	0.2500	0.6250	0.0321
32.0	2.3	0.2625	0.7750	0.0835
32.0	3.0	0.2625	0.9750	0.2624
32.0	4.0	0.2625	1.3625	0.9218
38.0	0.4	0.1625	0.4875	0.8413
38.0	0.8	0.1875	0.5375	0.1203

Table III-III (Continued):

F_D	F_e	α	λ	e_r
38.0	1.3	0.2125	0.6125	0.0054
38.0	1.7	0.2250	0.6250	0.0071
38.0	2.3	0.2375	0.7500	0.0527
38.0	3.0	0.2500	0.9500	0.1823
38.0	4.0	0.2500	1.300	0.8622
52.0	0.4	0.1125	0.6875	1.2535
52.0	0.8	0.1375	0.6500	0.3118
52.0	1.3	0.1625	0.6375	0.0598
52.0	1.7	0.1875	0.6625	0.0110
52.0	2.3	0.2125	0.7625	0.0057
52.0	3.0	0.2125	0.8625	0.1884
52.0	4.0	0.2500	1.3500	0.5107

SECTION III. NUMERICAL SIMULATION OF THE DISPERSION OF A DENSE EFFLUENT DISCHARGE INTO A HOMOGENEOUS STREAM (Texas A. and M. University)

TABLE III-IV

COEFFICIENTS FOR THIRD DEGREE POLYNOMIALS FOR α AND λ, EQ. (36)

(α)	(λ)
$A_{00} = 0.7121160$	$B_{00} = -0.004874467$
$A_{10} = -0.03598029$	$B_{10} = 0.003575079$
$A_{01} = 0.05137678$	$B_{01} = 0.5843794$
$A_{20} = 0.0007635895$	$B_{20} = 0.0004779123$
$A_{11} = 0.001468862$	$B_{11} = -0.02376157$
$A_{02} = -0.01879174$	$B_{02} = 0.04792207$
$A_{21} = -0.0000293576$	$B_{21} = 0.00005505273$
$A_{12} = 0.0003550325$	$B_{12} = 0.003477149$
$A_{30} = -0.000005716607$	$B_{30} = -0.0000040185666$
$A_{03} = -0.0007472655$	$B_{03} = -0.01916188$

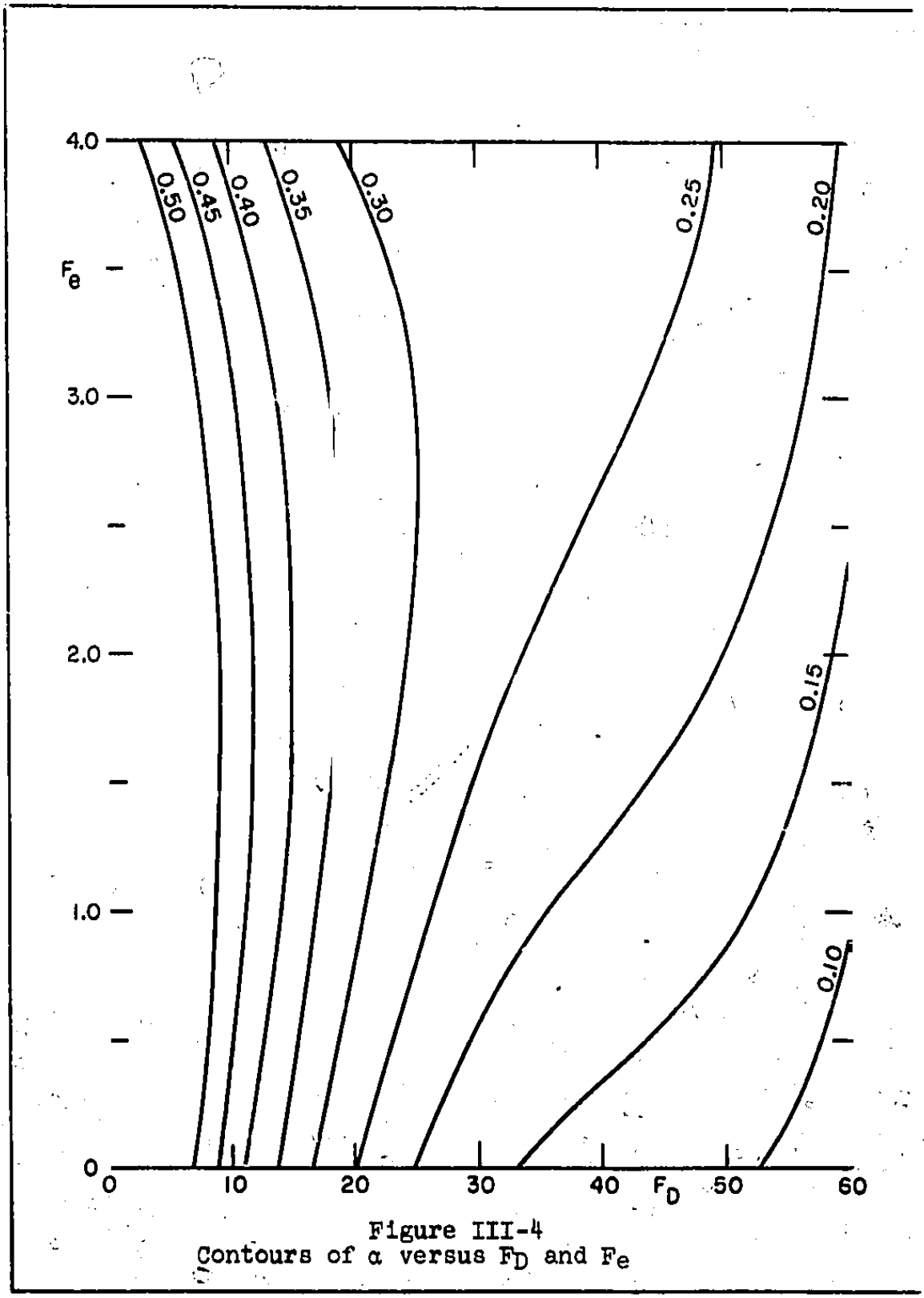

Figure III-4
Contours of α versus F_D and F_e

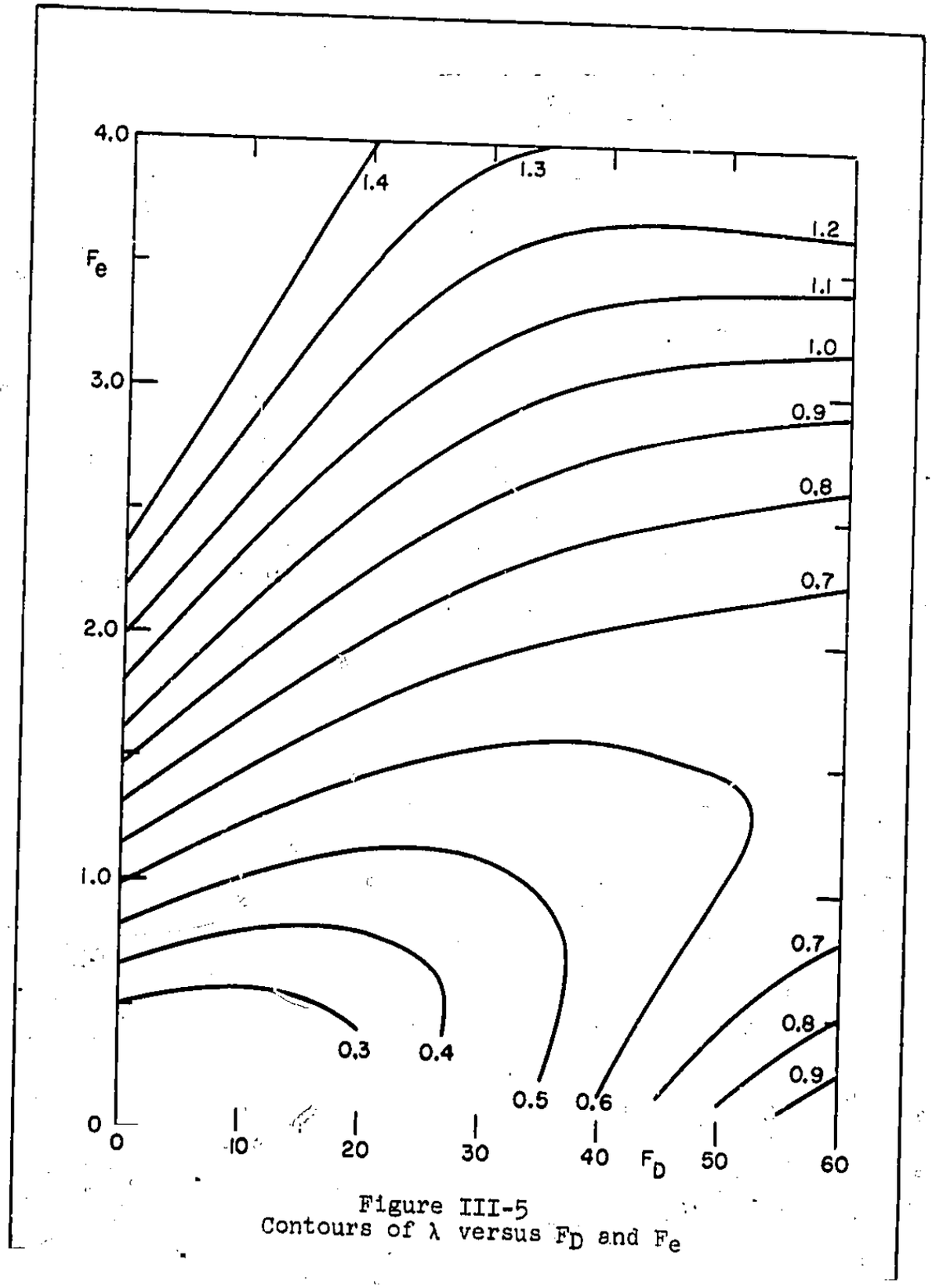

Figure III-5
Contours of λ versus F_D and F_e

SECTION III. NUMERICAL SIMULATION OF THE DISPERSION OF A DENSE EFFLUENT DISCHARGE INTO A HOMOGENEOUS STREAM (Texas A. and M. University)

TABLE III-V

MEAN VALUES AND STANDARD DEVIATIONS OF PERTINENT GEOMETRICAL AND DILUTION PARAMETERS AT THE CENTERLINE PEAK AS CALCULATED FROM THE NUMERICAL MODEL FOR THE JET REGIME USING POLYNOMIAL FITTED VALUES OF α and λ

	$(b/b_o)_m$	X_m^*	Z_m^*	(b/z)	V/U	S^*
Mean Values	37.0321	1.9637	2.3215	0.6760	1.0323	0.9323
Standard Deviations	9.4138	0.5432	0.3099	0.4321	0.0706	0.1613

SECTION III. NUMERICAL SIMULATION OF THE DISPERSION OF A DENSE EFFLUENT DISCHARGE INTO A HOMOGENEOUS STREAM (Texas A. and M. University)

Using the values of α,λ as given by the third degree polynomials, the numerical integration up to the peak of the jet axis was again carried out for each of the 49 combinations of F_D and F_e. Based upon this standard set of 49 cases, the mean values and standard deviations of the following quantities were computed: b/b_o, X_m^*, Z_m^*, S^*, $(b/Z)_m$ and $(V/U)_m$, where the m subscript refers to values at the maximum position of the jet axis. These values are given in Table III-V.

If we compare the mean values of X_m^* and Z_m^* derived from the WES data (Table III-I) with those derived from the numerical model (Table III-V) we see that there is good agreement for Z_m^* and reasonable agreement for X_m^* (particularly when it is considered that X_{am} is not as readily determined from the data as is Z_{am}). Moreover, we note from the standard deviations that the scatter of the computed values is less than that derived from the observed data. With regard to b/Z we note that its percent scatter is large compared with its counterpart ΔZ^* in Table III-I. Also, the ratio $\Delta Z/b$ derived from the two sets is only 1.36; one would expect this to be much larger. It would appear that the numerical model overestimates the value of b in the effort to yield a good simulation of dilution at the peak of the jet (last column of Table III-V). In fact, if one evaluates the mean value of b/b_o (with $b_o = D_o/2$) from the data of Table III-II (interpolated to position $x = x_m$), the result is approximately 17 with a standard deviation of 4. This mean value is less than half of the value derived from the numerical model.

Thus in summary, while the model gives a reasonable simulation of the geometry of the axis and of the dilution at the peak of the jet, it overestimates the lateral spreading factor. This would appear to indicate that the rendition of V, for which no actual data exists in the tests, is probably underestimated by the numerical model. Indeed an inspection of V/U at the peak of the jet as shown in Table III-V indicates a mean value close to unity and a scatter of values (as indicated by the standard deviation) such that V/U is less than unity for many cases. Physically this does not seem possible. However, our preliminary tests with all of the other numerical models indicates this same deficiency. Apparently there is still room for improvement in respect to the proper entrainment relation, particularly for a dense jet discharged into a stream.

SECTION III. NUMERICAL SIMULATION OF THE DISPERSION OF A DENSE EFFLUENT DISCHARGE INTO A HOMOGENEOUS STREAM (Texas A. and M. University)

As further testing of the numerical model, the latter has been employed in the attempt to simulate in more detail the geometrical configuration and dilution distribution in the jet regime for a number of tests selected from the WES flume experiments. The results are summarized in Appendix C.

G. Far Field Numerical Model

In the region downstream from the point of contact of the jet with the flume or sea bed the effluent is no longer in free fall but instead is forced to spread out laterally. The basic equations governing the flow and distribution of effluent are given for example by Crew (1970, Eqs. (2.2.1) to (2.2.4)). The analysis of these in their general form is quite complex. In order to simplify the analysis, we will make the following approximations:

a. The longitudinal (x-component) velocity within the region of the effluent is the same as that of the ambient stream (U), an approximation also made by Crew;

b. The pressure distribution in the vertical is assumed to be hydrostatic, vertical acceleration being neglected;

c. The sea surface is assumed to be level and at uniform atmospheric pressure;

d. Vertical mixing is allowed but lateral mixing is neglected;

e. A similarity hypothesis is employed in respect to the vertical distribution of concentration and outward velocity but not with respect to lateral distribution.

In respect to the last assumption, let C again represent the density anomaly $(\rho - \rho_e)/\rho_e$ and let v denote the lateral (y-component) velocity; we assume that

$$C = C_o F(z/h)$$

$$v = v_o F(z/h) \qquad (37)$$

where C_o, v_o and h each depends upon x and y for steady state conditions. It is assumed further that the function F goes to virtually zero at $z = H$ (the sea surface). This means that if F is a Gaussian form then the scale parameter h is much less than the depth H.

SECTION III. NUMERICAL SIMULATION OF THE DISPERSION OF A DENSE EFFLUENT DISCHARGE INTO A HOMOGENEOUS STREAM (Texas A. and M. University)

The vertically integrated equations of motion and continuity can be shown to take the following form:

$$U \frac{\partial (v_o h)}{\partial x} + N_1 \frac{\partial (v_o^2 h)}{\partial y} + N_2 \frac{\partial (g C_o h^2)}{\partial y} = 0 \qquad (38)$$

$$U \frac{\partial (C_o h)}{\partial x} + N_1 \frac{\partial (v_o C_o h)}{\partial y} = 0 \qquad (39)$$

$$U \frac{\partial (C_o^2 h)}{\partial x} + N_3 \frac{\partial (v_o C_o^2 h)}{\partial y} = -N_4 K C_o^2 h, \qquad (40)$$

where K is a vertical turbulent exchange coefficient (dimensions of length x velocity) and N_1, N_2, N_3 and N_4 are non-dimensional numbers which depend upon the form of the function $F(\zeta)$, where $\zeta = z/h$. In particular

$$\begin{aligned} N_1 &= \int_0^\infty F^2 \, d\zeta \Big/ \int_0^\infty F \, d\zeta \\ N_2 &= \int_0^\infty F \, \zeta \, d\zeta \Big/ \int_0^\infty F \, d\zeta \\ N_3 &= \int_0^\infty F^3 \, d\zeta \Big/ \int_0^\infty F^2 \, d\zeta \\ N_4 &= 2 \int_0^\infty \left(\frac{dF}{d\zeta}\right)^2 d\zeta \Big/ \int_0^\infty F^2 \, d\zeta \, . \end{aligned} \qquad (41)$$

The above equations are very similar to those given by O'Brien (1967) if one interprets the independent variable x/U as time. In O'Brien's analysis, a two-layer approximation is employed (corresponding to a "top hat" profile for F). In the analysis here, a Gaussian profile is assumed, i.e. $F(\zeta) = \exp(-\zeta^2)$. Moreover the initial distributions of v_o, C_o and h are taken as follows:

$$v_o = 0$$

$$C_o = E_1 \exp(-y^2/h_1^2) \qquad (42)$$

$$h = h_1$$

at $x = x_1$. The initial relation for C_o implies that the field of C is initially axially symmetric as in the jet regime ($x < x_1$). The relation between b and h_1 at $x = x_1$ is simply $h_1 = \sqrt{2}\, b$.

The exchange coefficient K is assumed to be given by

$$K = \beta\, Uh/N_1 \qquad (43)$$

where β is a non-dimensional coefficient which plays a role similar to α in the jet entrainment model.

In order to illustrate this far field numerical model, the following particular case was considered: $h_1 = 7$ ft., $E_1 = 2 \times 10^{-4}$, $U = 0.1$ kt and $\beta = 0.05$. Numerical integration based upon the characteristic form of (38) to (40) (see Appendix B) was carried out for 49 steps in x with $\Delta x = \Delta y = 1$ ft. Figure III-6 shows the contour $C = 0.2 \times 10^{-4}$ at different displacements downstream from x_1. Figure III-7 shows three different contours of C all at a distance of 49 ft. from x_1. The flattening and lateral spreading of the contours is quite similar to the distributions found in the WES tests for the far field. This illustration shows the importance of gravity in the spreading process even for very small density anomaly.

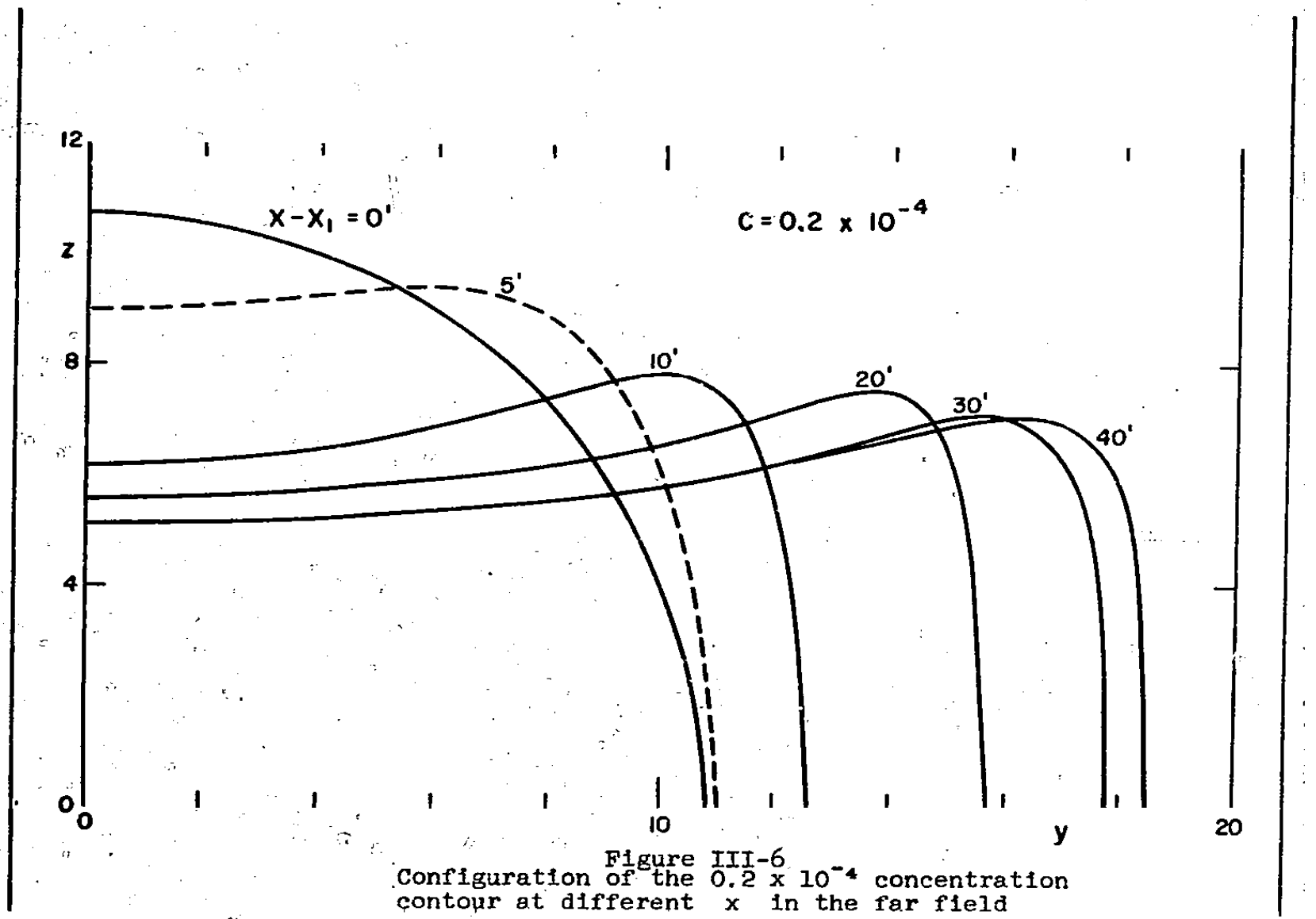

Figure III-6
Configuration of the 0.2×10^{-4} concentration contour at different x in the far field

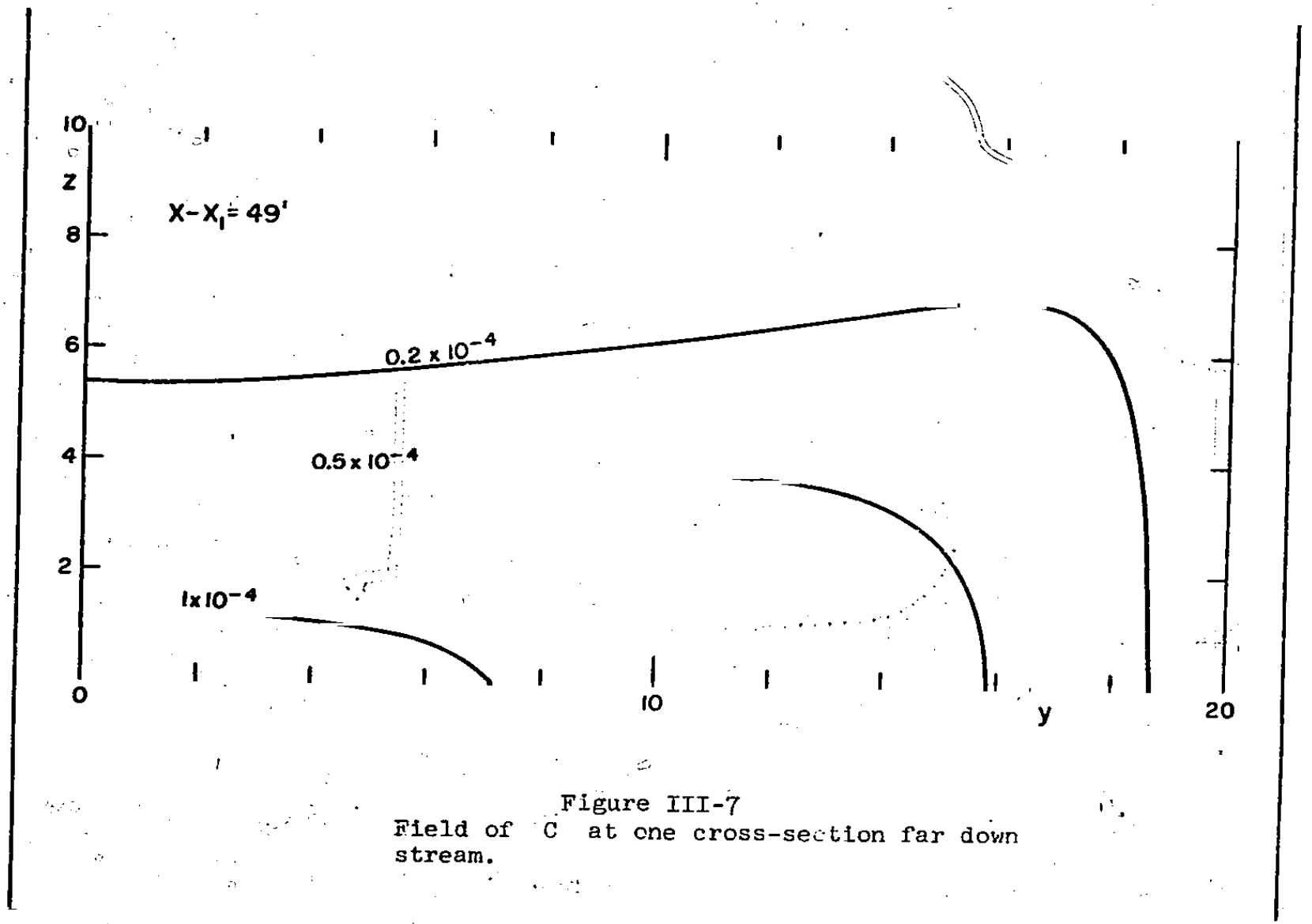

Figure III-7
Field of C at one cross-section far down stream.

SECTION IV. DESIGN CONSIDERATIONS

The effluent properties and flow rates from any size desalination plant, utilizing a distillation process, can be calculated for varying conditions of the performance ratio (R), and the concentration ratio (X_c). In Figure IV-1 is shown the density of the mixed effluent which is a function of performance ratio only. For an ambient temperature of 65°F and a 20°F temperature rise for the cooling water, the mixed effluent has a higher density than the receiving water for performance ratios above 6.

The criteria used for the design of a diffuser system was based on the dilution of the copper concentration to a value below 0.02 mg/liter. Assuming an average concentration of 0.65 mg/liter of copper in the brine blowdown and 0.06 mg/liter in the cooling water discharge, the copper concentration can then be estimated in the mixed effluent and the initial dilution required by the diffuser can be calculated. Figure IV-2 is a plot of $S_o(Cu)$ as a function of the performance ratio and the concentration ratio of a distaillation plant.

Similar plots can be produced for the dilution of the salinity of the effluent to within 5 percent of the receiving water and the temperature to 3°F above ambient. Salinity and temperature were found to require less dilution than that required for copper. The initial copper dilution in the vicinity of the outfall, $S_o(Cu)$ was therefore chosen as the criterion for the diffuser design.

A. Diffuser Design Based on Analysis of Inclined Dense Jets in Absence of Ambient Current (Dow, 1970)

Diffusers were designed to handle the effluents from 2, 5, 10, and 50 MGD desalination plants. For each value of X_c and R, the diffusers were designed for initital velocities of 5, 10, 15, and 20 feet per second, with diameter of ports of 0.25, 0.5 and 1.0 feet. For each case, a Froude number was calculated and the maximum height of a 60° angle jet computed. The number of ports required for each size of plant was then calculated.

Figure IV-3 is the resulting correlation of the maximum height (Z_m) of a 60° angle jet against Froude number (F_D) for different port diameters (D) and initial velocities (V_o) through the ports for a 10 MGD plant. The intersection of a D-line with a U_o-line represents a particular number of ports (n).

Figure IV - 1

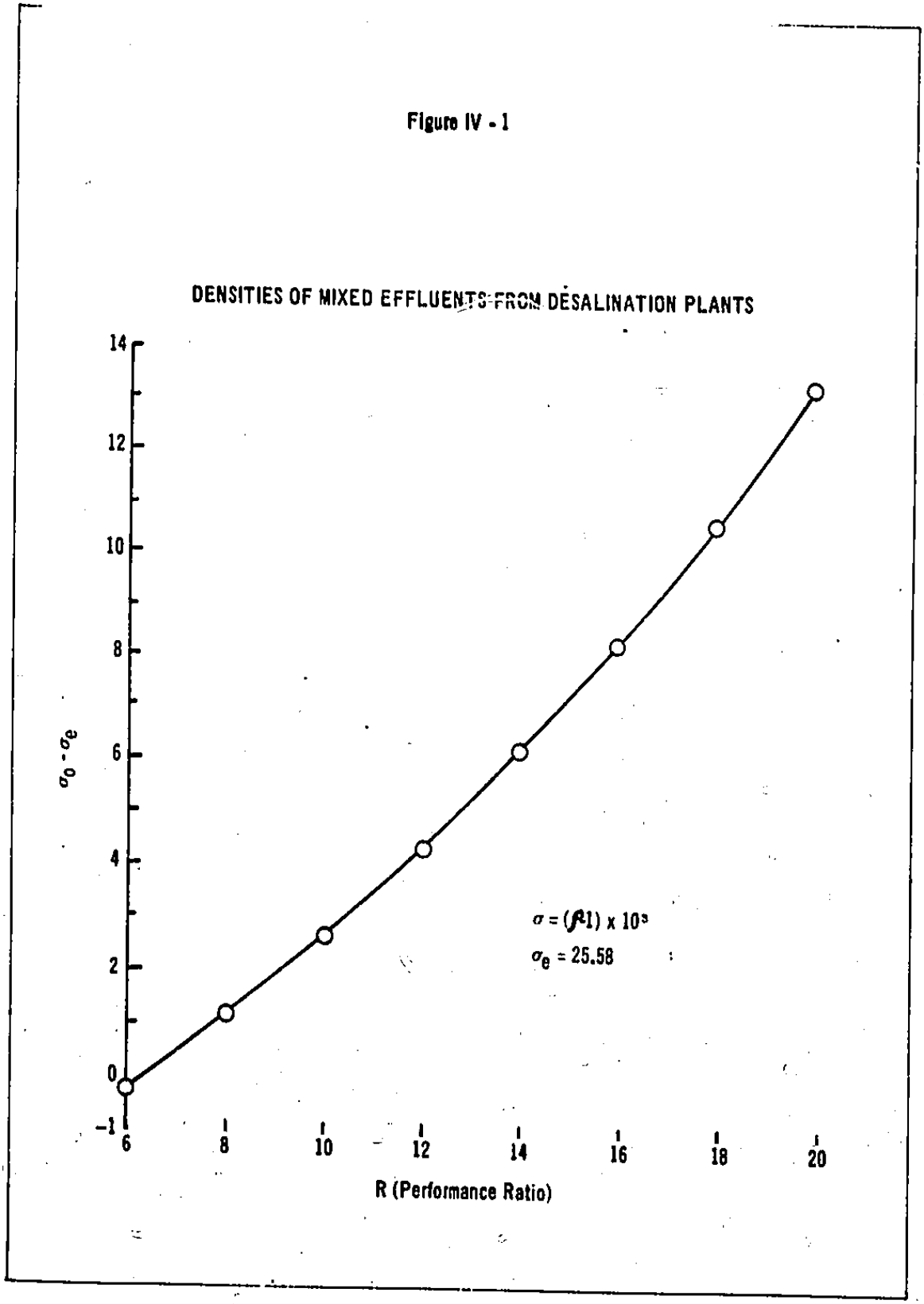
DENSITIES OF MIXED EFFLUENTS FROM DESALINATION PLANTS
$\sigma_0 - \sigma_e$
14
12
10
8
6
4
2
0
−1
6
8
10
12
14
16
18
20
R (Performance Ratio)
$\sigma = (\rho 1) \times 10^3$
$\sigma_e = 25.58$

Figura IV - 2

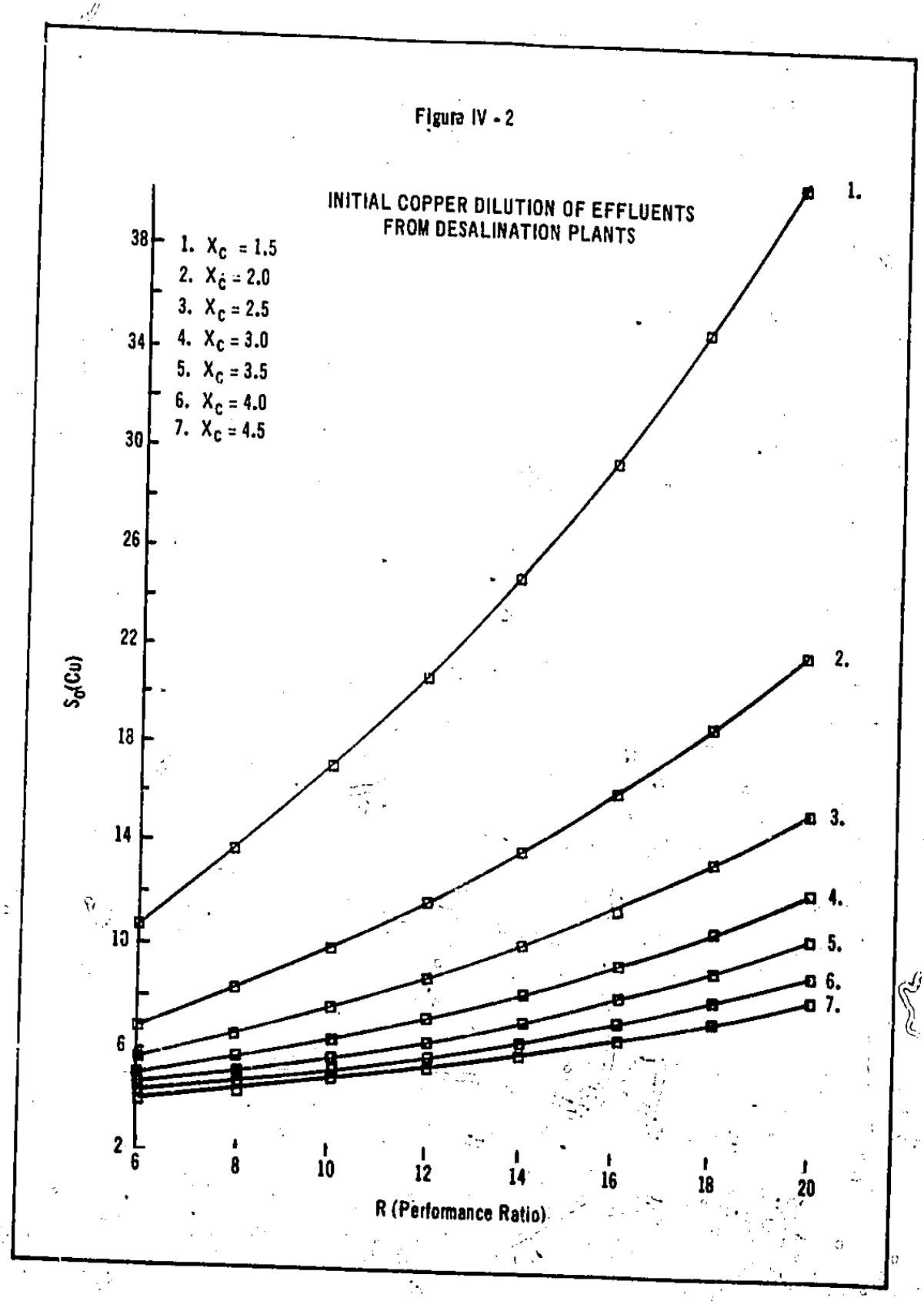
INITIAL COPPER DILUTION OF EFFLUENTS
FROM DESALINATION PLANTS
1. X_c = 1.5
2. X_c = 2.0
3. X_c = 2.5
4. X_c = 3.0
5. X_c = 3.5
6. X_c = 4.0
7. X_c = 4.5
S_o(Cu)
38
34
30
26
22
18
14
10
6
2
6
8
10
12
14
16
18
20
R (Performance Ratio)
1.
2.
3.
4.
5.
6.
7.

Figure IV - 3

10 MGD PLANT

X_c = 2.5; S_0(Cu) = 12; Effluent Flow Rate = 32.85 Cubic Feet/Second;

S. G. = 1.03395; Performance Ratio R = 16

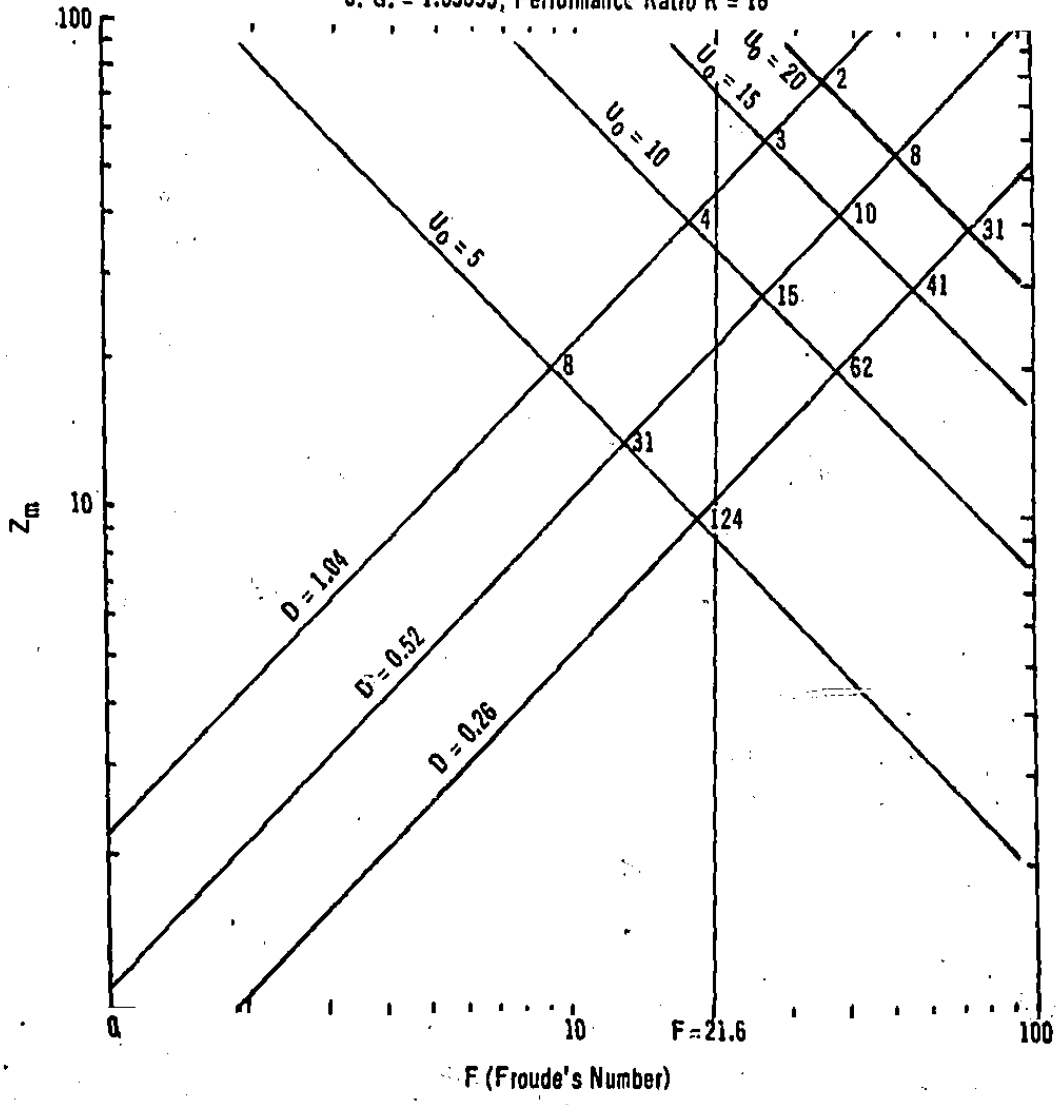

$S_0 = \frac{F}{1.8}$; $F_{min} = 1.8 \times 12 = 21.6$

The relationships of these values derived from the results of the dispersion of angled jets in a still fluid are:

$$D = \frac{Z_m}{2.04\ F_D} \tag{44}$$

$$U_o^2 = \frac{1}{2.04} (E_o g)\ F_D\ Z_m \tag{45}$$

$$n = \frac{4(2.04)^{5/2}}{\pi}\ Q_o\ F_D^{3/2}\ (E_o g)^{-1/2}\ Z_m^{-5/2} \tag{46}$$

If ports of other diameters or with other initial port velocities are selected, they can be inserted in the chart and the number of ports calculated from the following equation:

$$n = \frac{4\ Q_o}{\pi\ U_o D^2} \tag{47}$$

The minimum Froude number necessary to obtain the minimum required dilution of $S_o(Cu) = 12$ (from Figure IV-2 for the X_c and R chosen for this plant) is given by

$$S_o = F_D / 1.8 \tag{48}$$

This is the experimental value of dilution at the top of a 60° angled jet. This minimum value of F_D is represented by a vertical line in Figure IV-3. Any point on the right of this line will be an acceptable design meeting the copper dilution criterion.

The lateral spreading of the 60° angled jets at its maximum height was used to space the ports in the diffuser:

$$\text{Port Spacing} = 0.84\ F_D \times D \tag{49}$$

This spacing may result in an overlap of the multiple jets in their downward path after the required dilution has been reached.

Details of these calculations and the engineering of outfall systems for different size desalination plant have been published in the Office of Saline Water R & D Report No. 550 (Dow, 1970).

SECTION IV. DESIGN CONSIDERATIONS

B. Analyses of Dense Jets Discharged Upwards Into a Flowing Fluid

The flume study of the mixing characteristics of dense jets discharged vertically through a single and multiple port diffuser into a flowing fluid was carried out at the U. S. Army Corp of Engineer Waterways Experiment Station at Vicksburg, Mississippi. The results of this study have been published as Office of Saline Water R & D Report No: 714 and are compared with the numerical model developed in Section III.

Jet Geometry

The maximum height of the upper boundary of a jet, Z_m, was given by:

$$Z_m = 3.4 \times 10^{-0.148\ F_e} \times D_o\ F_D \qquad (50)$$

where Z_m represents the height above the port rather than of the flume floor.

Correlations of the lateral plume width with downstream distance led to the following equations for prediction of plume spread:

$$\frac{W}{W_o} = \left(\frac{X}{X_o}\right)^R \qquad (51)$$

where

X = distance downstream from diffuser, ft.
X_o = distance at which plume falls to bottom, ft
W = total plume width, ft.
W_o = plume width at $X = X_o$, ft.

and

$$R = 3.02 \times 10^{-0.26\ F_e} \quad \text{for } X \leq X_o \qquad (52)$$
$$R = 0.61 \log_{10} (4\ F_e) \quad \text{for } X > X_o \qquad (53)$$

The quantities X_o and W_o can be predicted by:

$$X_o = 9.62 \left(Z_m + D\right) \log_{10} \left(2\ F_e\right) \qquad (54)$$
$$W_o = 1.51 \left(Z_m + D\right) \log_{10} \left(4.91\ F_e\right) \qquad (55)$$

where D is the diameter of the diffuser pipe. The logarithmic correlations of equations (53) through (55) are limited to values higher than 1.0 inside the logarithm sign, which corresponds to F_e values higher than 0.25.

SECTION IV. DESIGN CONSIDERATIONS

The calibration of the model (Section III, E.) was carried out by fitting the data appropriate to the peak position of the axis of the jet (i.e., $x = X_m$ and $z = Z_{am}$). Equation (31) is rewritten for calculation of Z_{am}:

$$Z_{am} = 2.3 \times 10^{-0.148\ Fe} \times D_o\ F_D \qquad (56)$$

and

$$\Delta Z = 0.922\ Z_{am}$$

Since

$$Z_m = Z_{am} + 1/2\ (\Delta Z) \qquad (57)$$

$$= 1.461\ Z_{am}$$

then

$$Z_m = 3.36 \times 10^{-0.148\ Fe} \times D_o\ F_D \qquad (58)$$

This result is identical to the correlation expressed in equation (49). Either equation (49) or (57) could be used to calculate the maximum height of the upper boundary of a submerged dense jet discharged upwards into a flowing fluid.

The distance at which the jet reaches its maximum height is given by equation (30) which can be rewritten as follows:

$$X_m \equiv X_{am} = 1.778\ D_o\ F_D\ Fe^{1/2} \qquad (59)$$

Equations (53) and (54) are used to calculate the distance at which the jet falls to bottom in the direction of the current and the plume width at that point, respectively.

Jet Dilution

The correlation of the minimum dilution at downstream stations with the relevant dimensionless flow parameters was found to be a function of Fe and $\left(\frac{x}{X_o}\right)$ for the jet before and after falling to the bottom of the flume. This relationship is expressed as:

$$\varepsilon_m = 31 \times 10^{0.4\ Fe} \left(\frac{X}{X_o}\right)^{0.68} \qquad (60)$$

where

X = distance downstream from diffuser
X_o = distance at which plume falls to bottom
ε_m = minimum observed dilution

$$F_e = \frac{U}{V_o} \times F_D$$

The dilution as measured on the jet axis at the position Xam, corresponding to the maximum height Z_{am}, was fitted by the empirical relation represented in Section III of this report as equation (33):

$$S = 18\, e^{0.8\, F_e} \qquad (33)$$

C. Diffuser Design for Desalination Plants

Examples of desalination plants of different sizes with varying concentration and performance ratios, chosen to demonstrate the practical application of the design procedure, are given below: (Dow, 1970)

2 MGD Plant:

Concentration Ratio, X_c	= 1.5
Performance Ratio, R	= 12
Mixed Effluent Flow Rate	= 9.86 cu.ft./sec.
	= 4425 gallons/min.
Specific Gravity of Effluent	= 1.02998

5 MGD Plant:

Concentration Ratio, X_c	= 2.0
Performance Ratio, R	= 14
Mixed Effluent Flow Rate	= 19.94 cu.ft./sec.
	= 8954 gallons/min.
Specific Gravity of Effluent	= 1.03185

10 MGD Plant

Concentration Ratio, X_c	= 2.5
Performance Ratio, R	= 16
Mixed Effluent Flow Rate	= 32.85 cu.ft./sec.
	= 14,744 gallons/min.
Specific Gravity of Effluent	= 1.03395

50 MGD Plant

Concentration Ratio, X_c	= 3.0
Performance Ratio, R	= 18

SECTION IV. DESIGN CONSIDERATIONS

Mixed Effluent Flow Rate	= 136.8 cu.ft./sec. = 61,410 gallons/min.
Specific Gravity of Effluent	= 1.03633

Ambient design conditions of the seawater are taken as:

Concentration Ratio	= 1.0 (35,000 ppm TDS)
Temperature	= 65°F

The temperatures of the product water, brine blowdown, and cooling water discharge are all chosen to be 85°F... 20°F higher than ambient.

The design of the diffuser for a 10 MGD plant, based on the 60° angled jet in a still fluid, is shown in Figure IV-3. With a port diameter, D_o, of 0.52 feet and an initial velocity through the port, V_o of 10 feet/second, the Froude number F_D = 26.4 and the dilution at the maximum height of the jet (Z_m = 28 feet) will be

$$S_o = \frac{F_D}{1.8} = 14.7$$

For these same conditions, and in the presence of an ambient steady current, U, the developed equations for a vertical jet, equations (50) through (60) and equation (33) are used to calculate the geometry of the jet and the dilution downstream from the diffuser. The results of these calculations are given in Table IV-I and plotted in Figures IV-4, 5, and 6.

The dimensions of the jets, as a function of the ambient current, may be calculated using the developed equations as listed below:

Z_m	equation (50) or (58)
X_m	equation (59)
X_o	equation (54)
W_o	equation (55)
W_m	equation (51) and (52)
S	equation (33)
ε_m at X_o and X_m	equation (60)

In the absence of current (U = o) the maximum height of a 60° angled jet, Z_m, and the dilution at that point, S, were calculated using equations (44) and (48) respectively, while the lateral spread of the jet at its maximum height W_m may be calculated, using the port spacing from equation (49).

TABLE IV-I

JET GEOMETRY AND DILUTION IN THE PRESENCE OF AN AMBIENT CURRENT FOR THE 10 MGD PLANT

Ambient Current U Knots	$\frac{U}{V_o}$	$F_e = \frac{U}{V_o} \times F_D$	Z_m ft.	X_m ft.	X_o ft.	W_o ft.	W_m ft.	S at $X=X_m$	ε_m at $X=X_o$	ε_m at $X=X_m$
0	0	0	28	--	--	--	11.5	14.7	--	--
0.1	0.446	0.446	40	16.3	--	20.6	--	25.7	46.8	--
0.2	0.892	0.892	34.4	23.1	83.2	33.3	3.5	36.7	70.5	29.5
0.3	1.338	1.338	29.6	28.2	121.7	36.5	5.0	52.5	106.3	39.3
0.4	1.785	1.785	25.4	32.6	135.0	36.1	8.3	75.1	160.5	61.1
0.5	2.231	2.231	21.8	36.5	136.2	34.2	12.0	107.3	242.0	98.8
0.6	2.677	2.677	18.7	39.9	131.0	31.6	15.3	153.2	365.0	162.6

$E_o = \frac{\rho_o - \rho_e}{\rho_e} = 0.0088$

D_o = 0.52 feet

V_o = 10 feet/second

F_D = 26.4

Figure IV-4

DIMENSIONS OF JETS INJECTED UPWARDS INTO A FLOWING FLUID FOR A 10-MGD DESALINATION PLANT

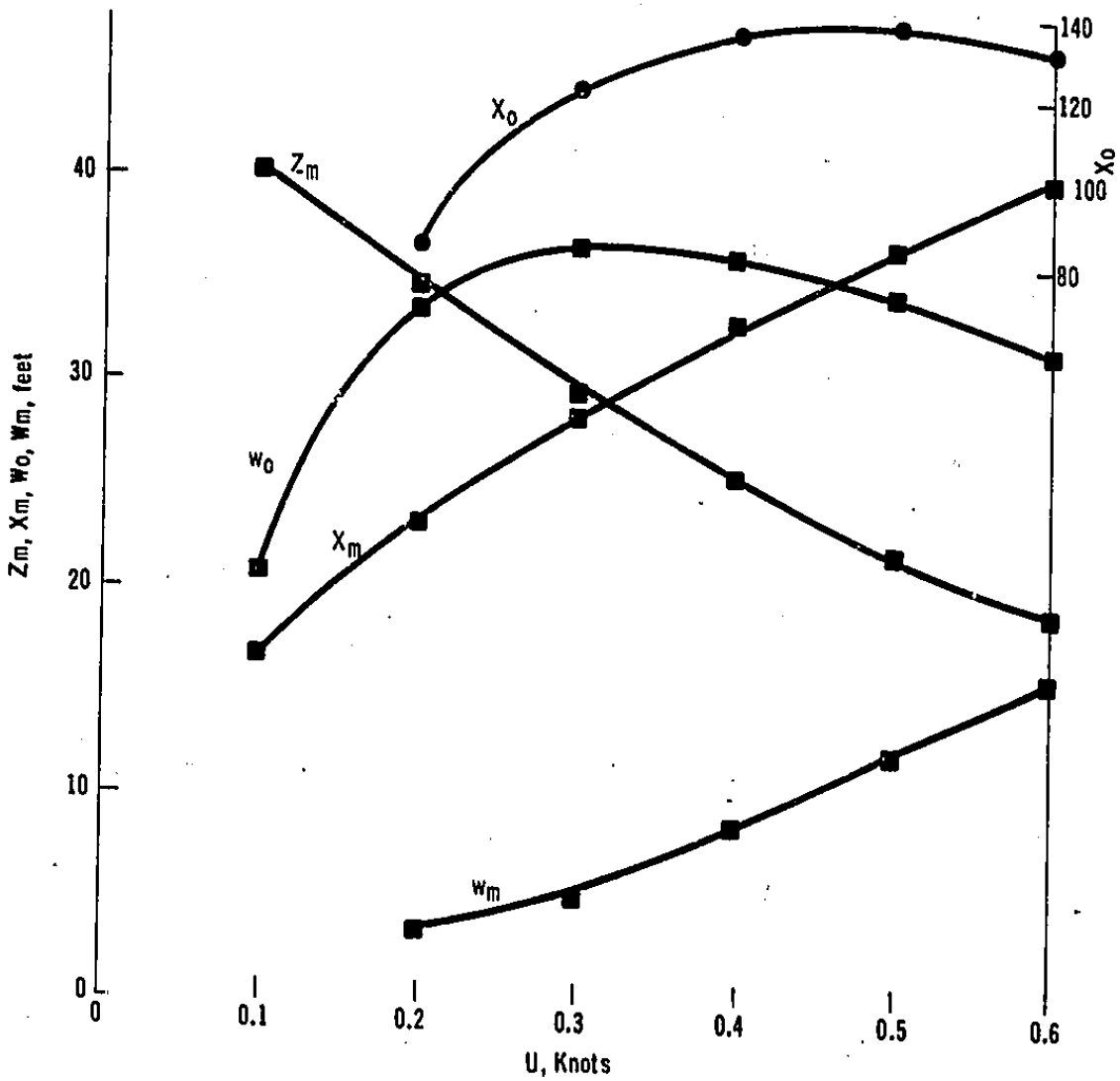

Figure IV-5

DILUTION IN JETS INJECTED UPWARDS INTO A FLOWING FLUID FOR A 10-MGD DESALINATION PLANT

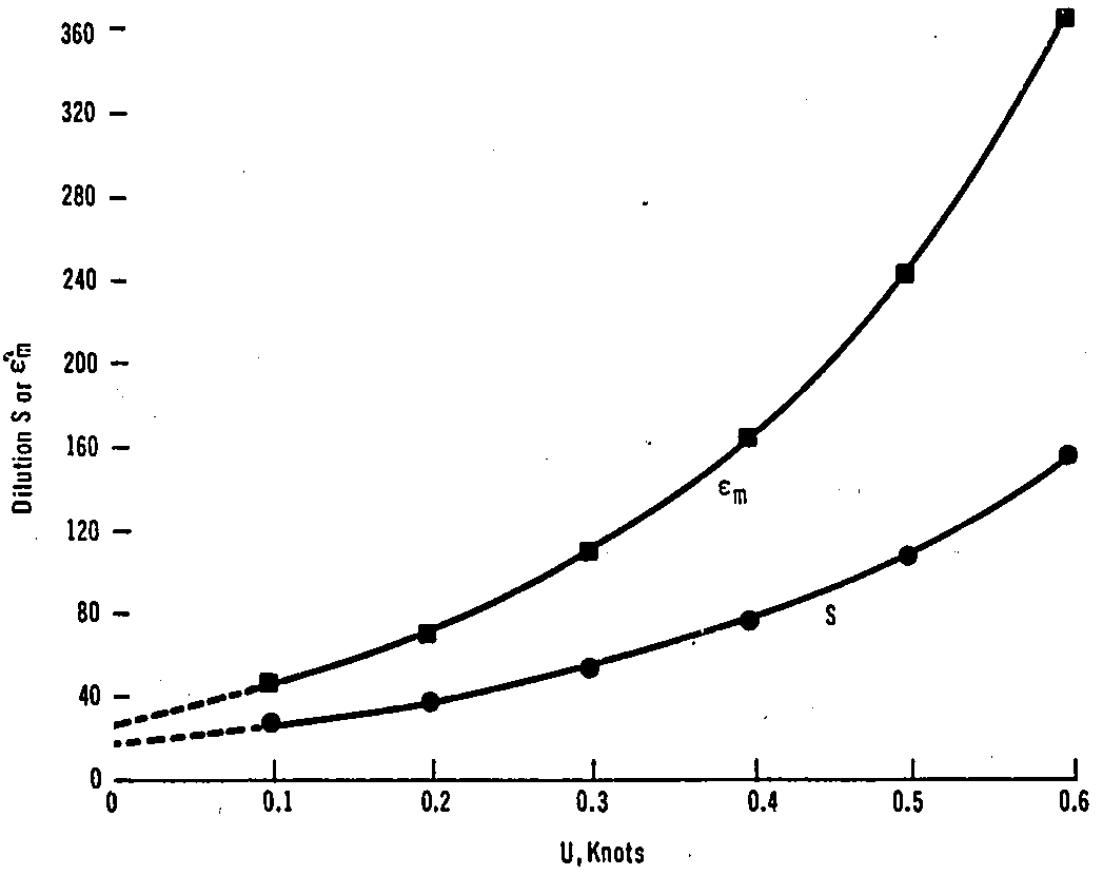

Figure IV-6

DIAGRAMATIC REPRESENTATION OF JETS INTO FLUID FLOWING AT VARIOUS SPEEDS FOR A 10-MGD DESALINATION PLANT

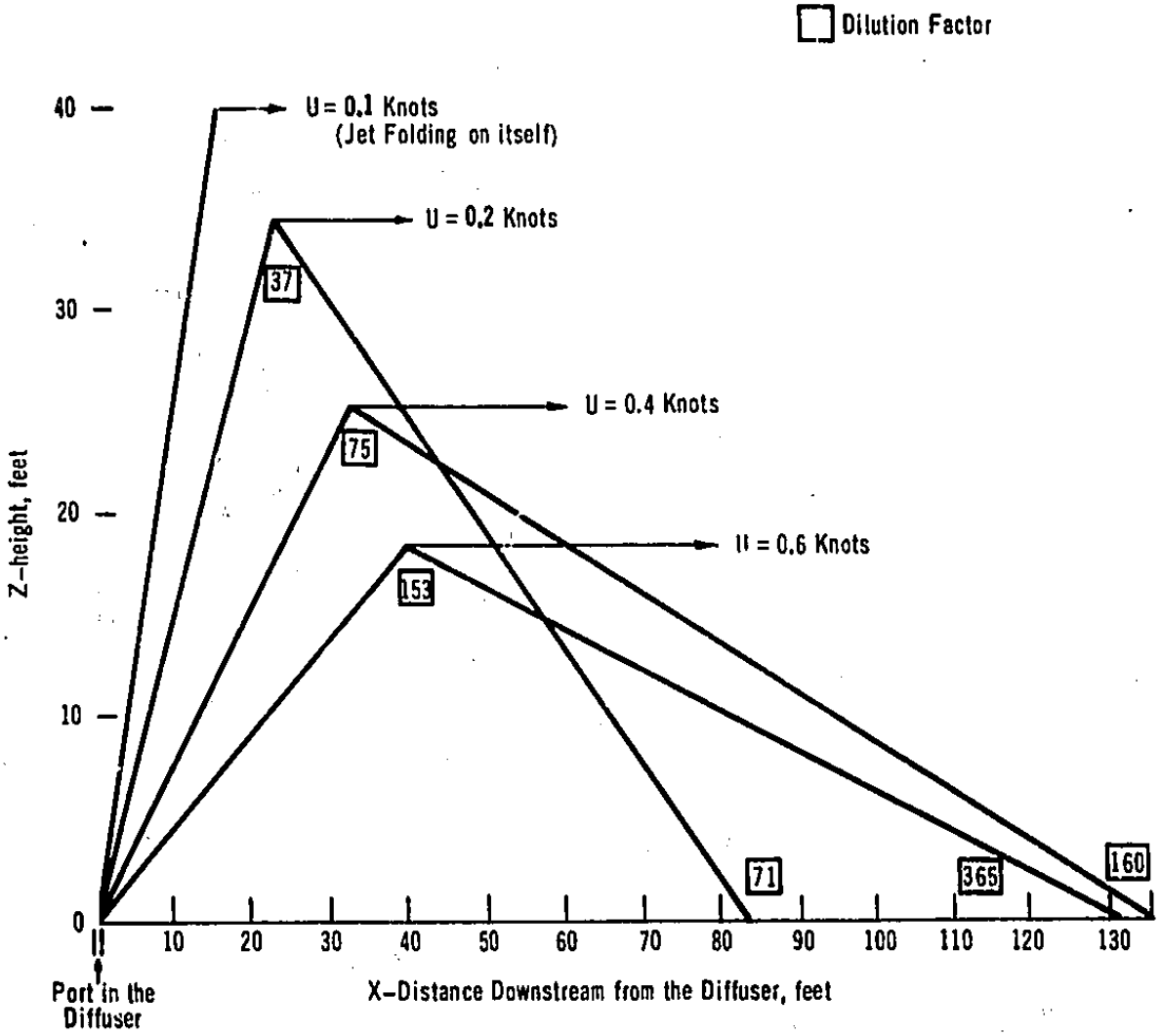

SECTION IV. DESIGN CONSIDERATIONS

The predicted dilutions in the presence of an ambient current are higher than the design value of 14.7 obtained from the analysis of a 60° angled jet in a still fluid. The width of the jet at its maximum height, to be used as the minimum port spacing, W_m, is less than or equal to the design value for ambient currents up to 0.5 knots.

The diffuser designs for 2, 5, 10, and 50 MGD distillation desalination plants, are summarized in Table IV-II, along with the jet geometry and jet dilution calculated in the presence of an ambient current of 0.2 knots.

The design procedure, developed from the analysis of 60° angled jets in still fluid, represents an extreme condition, and thus may be considered to be a conservative design. Since the cost of the diffuser is a minor part of the outfall pipe line, no appreciable savings could be accomplished by reducing the diffuser length or the number of ports.

TABLE IV-II

JET GEOMETRY AND DILUTION IN PRESENCE OF AN AMBIENT CURRENT OF 0.2 KNOTS FOR DIFFERENT SIZE DESALINATION PLANTS

Plant Size MGD	Effluent Properties		Diffuser Design			Jet Geometry			Jet Dilution	
	Flow cu.ft./sec	$E_o = \frac{\rho_o - \rho_e}{\rho_e}$	D_o ft.	V_o ft/sec	n (no. of ports)	Z_m ft.	X_m ft.	X_o ft.	S at $X=X_m$	ε_m at $X=X_o$
2	9.86	0.0048	0.25	10	20	24.8	30	122	70	148
5	19.95	0.0067	0.375	10	19	37.5	27.8	112	40	80
10	32.85	0.0088	0.50	10	16	34.4	23.1	83.2	37	71
50	136.8	0.0110	0.75	10	26	39.4	21.0	45.4	31	57

SECTION V. ACKNOWLEDGEMENT

The experimental investigations published as Parts I and II of this report were conducted at the U. S. Army Corp of Engineer Waterways Experimental Station at Vicksburg, Mississippi.

The numerical model analysis was performed by Professor R. O. Reid and T. M. Mitchell of the Department of Oceanography, Texas A & M University.

The coordination of the data reduction and application to outfall designs was performed by Dr. M. A. Zeitoun and W. F. McIlhenny of The Dow Chemical Company.

The cooperation of the following personnel of the Waterways Experiment Station is acknowledged:

Mr. H. B. Simmons - Chief of the Hydraulics Division
Mr. T. E. Murphy - Chief of the Structure Branch
Mr. F. A. Herrmann - Chief of the Estuaries Branch

and Messrs. R. A. Boland Jr., W. H. Bobb, F. M. Holly, Jr. and J. L. Grace, Jr.

SECTION VI. BIBLIOGRAPHY

Abraham, G., 1967: "Jets with Negative Buoyancy in Homogeneous Fluid". Journal of Hydraulic Research, 5 (4), 235-248.

Abramovich, G. N., 1963: "The Theory of Turbulent Jets", Tranlation by Scripta Technica, MIT Press.

Burchett, M. E., G. Tchobanaglous, and A. J. Burdoin, 1967: "Submarine Outfall Calculation". Public Works, pp. 95-101.

Crew, Henry, 1970: "A numerical model of the dispersion of a dense effluent in a stream". Technical Report 70-10T, Project 716, Texas A. and M. University, 156 pp.

Csanady, G. T., 1965: "The buoyant motion within a hot gas plume in a horizontal wind". J. Fluid Mechanics, Vol. 22, 225-239.

Dow Chemical Company, 1967: "A Study of the Disposal of the Effluent from a Large Desalination Plant". Office of Saline Water, Research and Development Report No. 316.

, 1968: "Disposal of the Effluents from Desalination Plants into Estuarine Waters". Office of Saline Water, Research and Development Report No. 415.

, 1969: "Disposal of the Effluents from a large Desalination Plant; The Effects of Copper, Heat, and Salinity". Office of Saline Water, Research and Development Report No. 437.

, 1970: "Conceptual Designs of Outfall Systems for Desalination Plants". Office of Saline Water, Research and Development Report No. 550.

Fan, Loh-Nien, 1967: "Turbulent buoyant jets into stratified or flowing ambient fluids". Report No. KH-R-15, W. M. Keck Laboratory of Hydraulics and Water Resources, California Institute of Technology, 429 pp.

Fox, D. G., 1969: "The Forced Plume in a Stratified Fluid" NCAR Manuscript 68-197, National Center for Atmospheric Research, 51 pp.

, 1970: "Forced plume in a stratified fluid". Journal of Geophysical Research, vol. 75, 6817-6835.

Hirst, E. A., 1971: "Analysis of round turbulent, buoyant, jets discharged to flowing ambients". Report ORNL-4685, Oak Ridge National Laboratory, 37 pp.

SECTION VI. BIBLIOGRAPHY

Keffer, J. F. and W. D. Baines, 1963: "The round turbulent jet in a cross-wind". J. Fluid Mechanics, Vol. 15, 481-496.

Lawrence, C. H., 1962: "Sanitary Considerations of a Five-Mile Ocean Outfall". Trans. Am.Soc. of C. E., 127, pp. 294-325.

Morton, B. R., 1961: "On a momentum-mass flux diagram for turbulent jets, plumes and wakes". J.Fluid Mechanics, Vol. 10, 101-112.

O'Brien, James J., 1967: "The non-linear response of a two-layer, baroclinic ocean to a stationary, axially-symmetric hurricane, Part II. Upwelling and mixing induced by momentum transfer". Journal of Atmospheric Sciences, Vol. 24, 208-215.

Pearson, E. A., 1956: "An Investigation of the Efficacy of Submarine Outfall Disposal of Sewage and Sludges". California State Water Pollution Control Board, Publication 14, Sacramento.

Pratte, B. D. and W. D. Baines, 1967: "Profiles of the round turbulent jet in a cross flow". Journal of the Hydraulic Divison, HY6, Vol. 93, 53-64.

Rawn, A. M., F. R. Bowerman, and N. H. Brooks, 1960: "Proceedings Paper 2424, J. San. Eng. Division, Am. Soc. of C. E., 86, 65-105.

Turner, J. S., 1966: "Jets and Plumes with Negative or Reversing Buoyance". J. Fluid Mech., 26, (4), 779-792.

U. S. Army Engineer Waterways Experiment Station, 1971: "Model Studies of outfall systems for Desalination Plants, Part I: Flume study of the mixing characteristics of dense jets discharged into a flowing fluid". Office of Saline Water, Research and Development Report No. 714.

, 1971: "Model Studies of Outfall systems for Desalination Plants. Part II: Tests of Effluent Dispersion in Selected Estuary Models". Office of Saline Water, Research and Development Report No. 736.

Zeitoun, M. A., W. F. McIlhenny, and R. O. Reid, 1969: "Disposal of Effluents from Desalination Plants". Chem. Eng. Prog., Symposium Series Vol. 65, No. 97, 156-166.

Zeitoun, M. A., W. F. McIlhenny, 1971: "Conceptual Designs of Outfall Systems for Desalination Plants" Reprint 1971 Offshore Technology Conference publication, April 18, 1971.

SECTION VII. APPENDIX A. LIST OF SYMBOLS

b	lateral scale parameter
C	concentration of effluent, $(\rho - \rho e)/\rho e$
C_d	drag coefficient
D	port displacement above the flume floor
D_o	port diameter
E	axial value for effluent concentration
E_o	effluent concentration at the port
F_D	densimetric Froude number at the port
F_e	Froude number based on the ambient flow
f_n	effective lateral force per unit length acting normal to the jet axis
g	acceleration due to gravity
h	vertical scale parameter (far field model)
J	non-dimensional momentum flux
K	vertical exchange coefficient
M	non-dimensional volume flux
q_e	volume of entrainment per unit arc length per unit time
r	radial distance from the jet axis
S	non-dimensional axial dilution function
s	arc length along the jet axis
U	ambient current
V	effective axial conveyance velocity
V_o	jet velocity at the port
v	lateral (y-component) velocity
X_{am}	x coordinate corresponding to the peak of the experimental jets

SECTION VII. APPENDIX A. LIST OF SYMBOLS

X_m^*	non-dimensional quantity associated with the x coordinate of the experimental jet axis peak
x	downstream coordinate
y	lateral coordinate
Z_{am}	maximum z coordinate (above the port) of the experimental jet axes
Z_m^*	non-dimensional quantity associated with the z coordinate of the experimental jet axis peak
z	vertical coordinate, positive upwards
α	non-dimensional entrainment coefficient
$\alpha_1, \alpha_2, \alpha_3$	non-dimensional entrainment coefficient
β	non-dimensional exchange coefficient, Eq. (43)
γ	non-dimensional constant
ΔZ	width of the experimental jets, vertical direction
ΔZ^*	non-dimensional quantity associated with the width of the experimental jets
ΔC	incremental arc length used in numerical integration
ε	effluent dilution at any point in the jet
ε_{min}	minimum dilution (axial) at a given jet cross-section
ζ	non-dimensional arc length along the jet axis
η	non-dimensional coordinate in the z direction

SECTION VII. APPENDIX A. LIST OF SYMBOLS

θ	angle between a tangent to the jet axis and the horizontal
λ	non-dimensional coefficient - depends upon the form of the distribution profile
ξ	non-dimensional coordinate in the x direction
ρ_e	environmental density
ρ_m	local axial density of the jet
ρ_o	initial density of the effluent at the port

SECTION VII. APPENDIX B. CHARACTERISTIC FORM FOR THE FAR FIELD MODEL

With K taken as in (43) and with N_3 taken equal to N_1 as an approximation (simplifies the resulting relations), it can be shown that (38), (39), and (40) can be put in the following characteristic form:

$$\frac{d}{dx}(v_o + 2Q) + \frac{Q}{2}\frac{dL}{dx} = -\frac{\alpha}{h}(v_o - \frac{1}{2}Q)$$

$$\text{along } \frac{dy}{dx} = \frac{N_1}{U}(v_o + Q) \qquad \text{(B-1)}$$

$$\frac{d}{dx}(v_o - 2Q) - \frac{Q}{2}\frac{dL}{dx} = -\frac{\alpha}{h}(v_o + \frac{1}{2}Q)$$

$$\text{along } \frac{dy}{dx} = \frac{N_1}{U}(v_o - Q) \qquad \text{(B-2)}$$

and

$$\frac{dL}{dx} = \frac{\alpha}{h} \text{ along } \frac{dy}{dx} = \frac{N_1 v_o}{U} \qquad \text{(B-3)}$$

where

$$Q = \left(2\frac{N_2}{N_1} g C_o h\right)^{1/2}$$

$$L = \ln C_o \qquad \text{(B-4)}$$

For the Gaussian profile in the vertical, $N_1 = 1/\sqrt{2}$ and $N_2 = 1/\sqrt{\pi}$.

The numerical integration procedure with similar equations is described by O'Brien (1967). One predices v_o, Q, L versus y at a new position, $x + \Delta x$, downstream from the distribution versus y at x. The variables C_o and h are easily evaluated from L and Q using (B-4).

SECTION VII. APPENDIX C. COMPARISON OF THE NUMERICAL MODEL WITH THE WES FLUME EXPERIMENTS

To test the ability of the numerical model to accurately predict the geomtrical configuration and dilution distributions in the jet regime, the model was run to simulate the results of some of the WES experiments. For both sets of tests (geometry and dilution), input to the model consisted of the appropriate values of D_o, F_D, and F_e. The required values of α and λ were calculated using the third degree polynomial mentioned earlier.

Values of the lateral scale parameter, b, the dilution ratio, E_o/E, and the s, x, and z coordinates of the centerline were calculated for the entire jet regime (from the port to the point, x_c, where the centerline reached the flume floor, see Figure III-2). The three coordinate values were calculated in feet so that the jet centerline and the dilution ratios could be compared directly with the experimental results given in ghe Appendix of Part I of the WES report.

The experiments chosen for simulation of the geometrical configurations are listed in Table VII-I. Two different groups of test conditions were selected: (1) constant F_e and increasing F_D; (2) constant F_D and increasing F_e.

Figures VII-1a through VII-1e show the comparison for the sequence of geometry tests with increasing F_D (with constant F_e). The x and z coordinates of the centerline peak increase with increasing F_D (as one would expect) and x_c also increases with increasing F_D (as should also be expected). The predicted centerline position is considered reasonably good for the portion of the jet from the port to the peak for all five cases. For the portion of the jet past the peak, the centerline position is good in only two of the intermediate cases--for the low F_D the centerline is too high, while it lies practically on the lower boundary of the jet for the two highest values of F_D. This good agreement for the rising part of the jet and poor agreement in the falling portion is probably due in large measure to the fact that the model was calibrated using values at the peak, with no consideration of the portion of the jet past the peak. Part of the problem may also be due to inaccuracies in sketching the boundaries of the experimental jets. Note particularly in tests 309 (Figure VII-1c) and 311 (Figure VII-1d) that the boundaries spread very little on the falling portion of the jet.

Figures VII-2a through VII-2d summarize the geometry comparison for the test sequence with increasing F_e (constant F_D).

SECTION VII. APPENDIX C. COMPARISON OF THE NUMERICAL MODEL WITH THE WES FLUME EXPERIMENTS

TABLE VII-I

Experiments used for Simulation of the Geometrical Configurations

Test No.	F_e	F_D
307	0.8879	18.8
308	0.8879	24.5
309	0.8879	29.8
311	0.8879	41.4
313	0.8879	52.4
304	0.4440	35.5
310	0.9323	35.5
317	1.3763	35.5
331	2.1311	35.5
345	4.4397	35.5

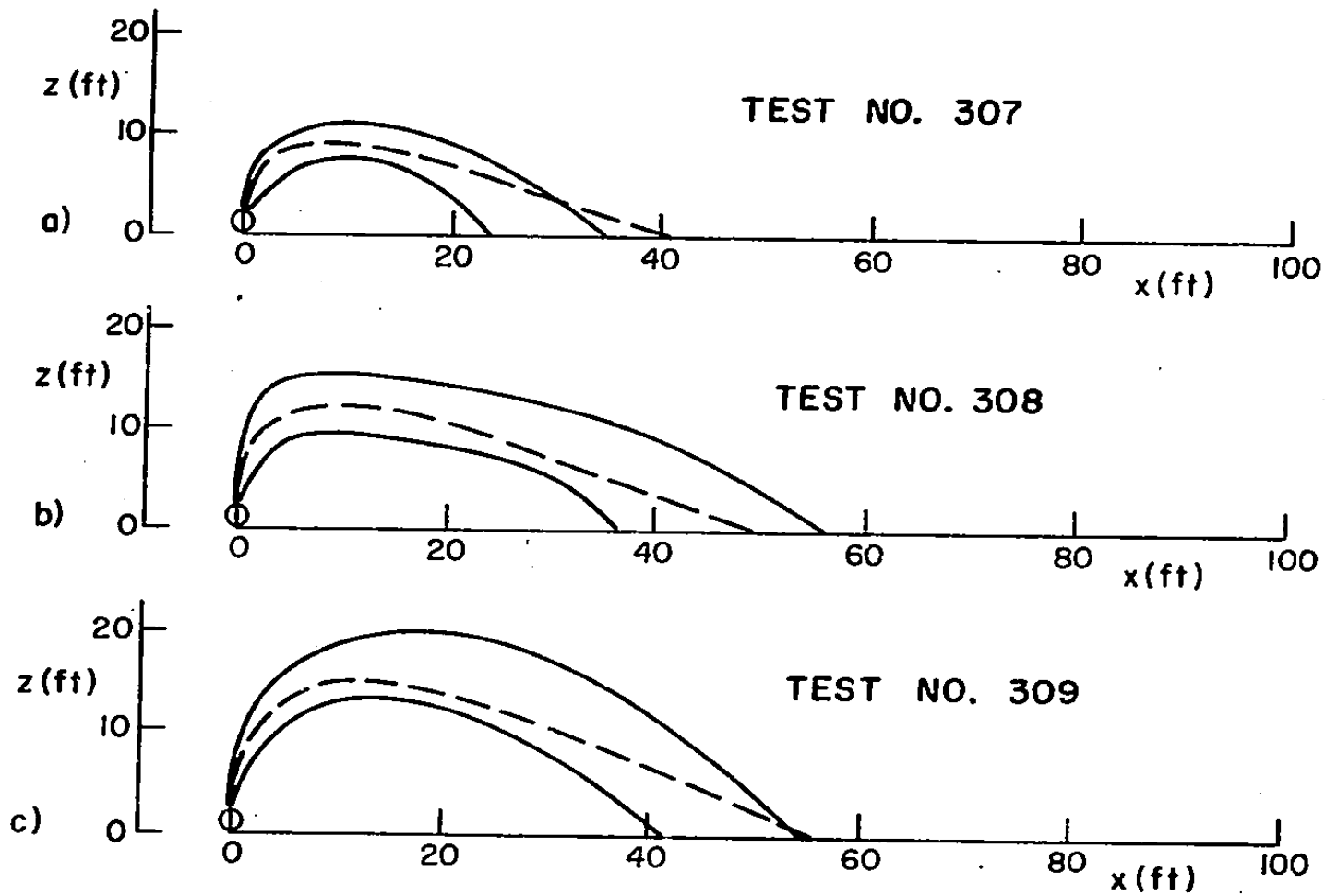

Figure VII-1
Comparison of experimental and model geometries for constant F_e and increasing F_D

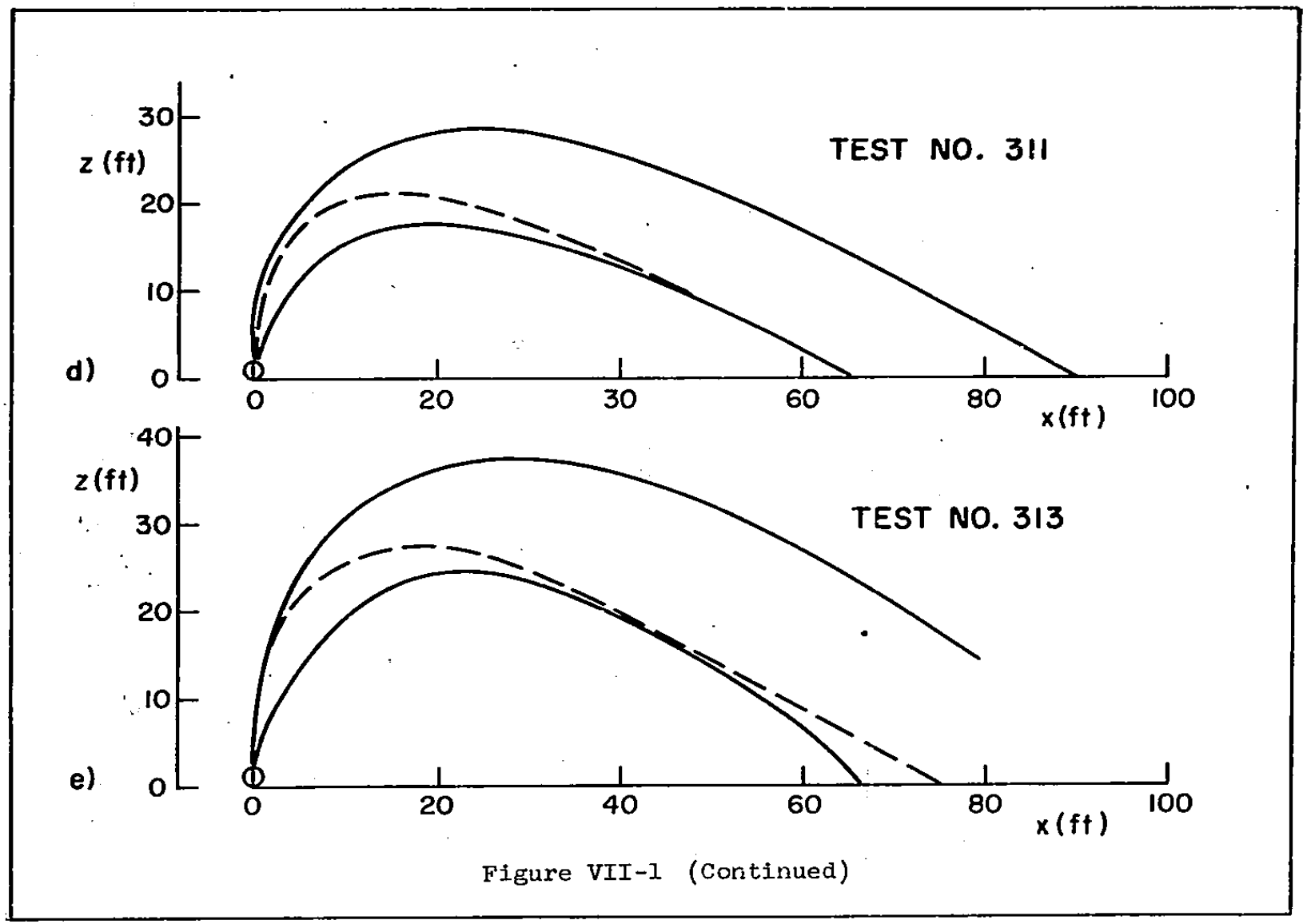

Figure VII-1 (Continued)

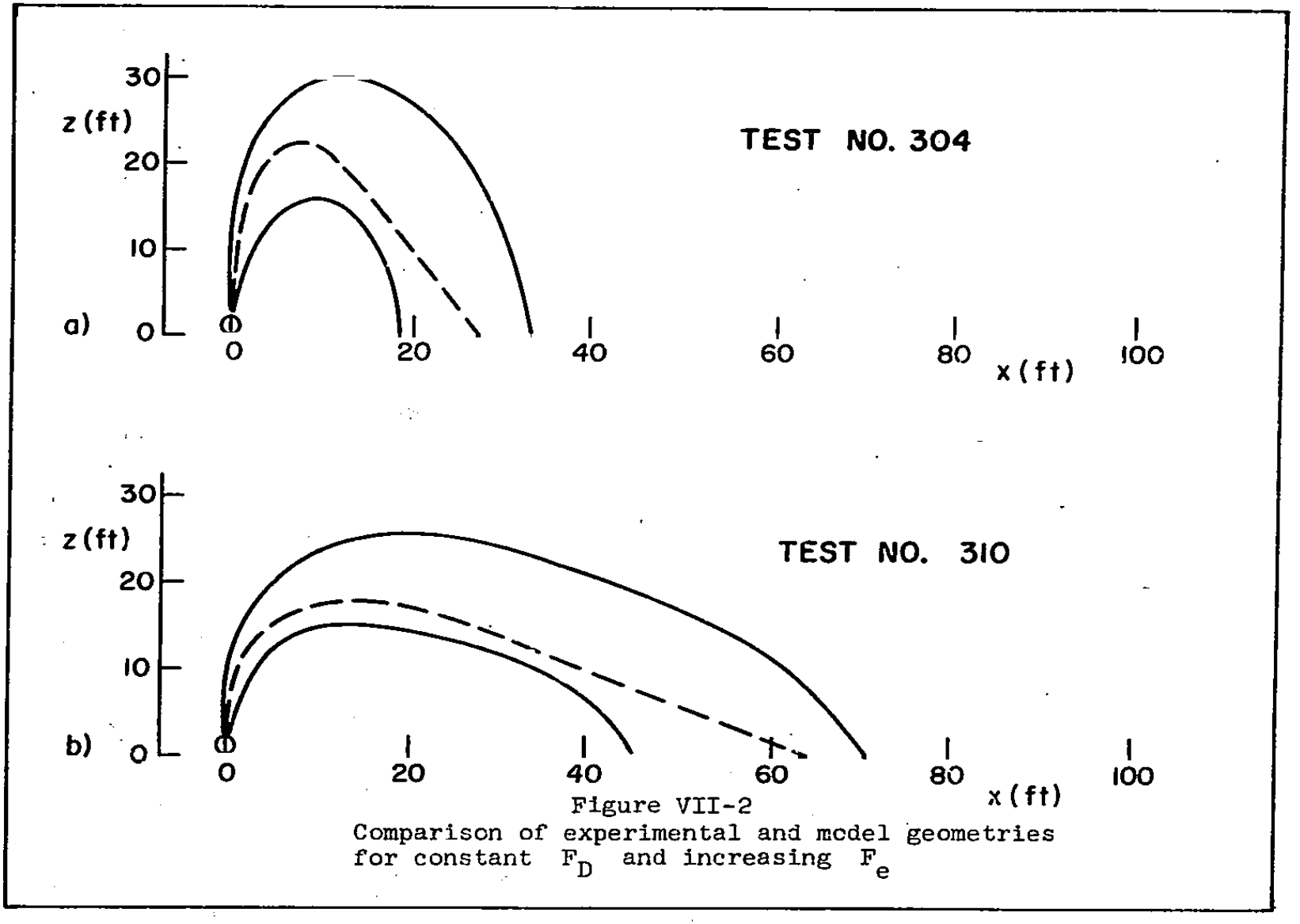

Figure VII-2

Comparison of experimental and model geometries for constant F_D and increasing F_e

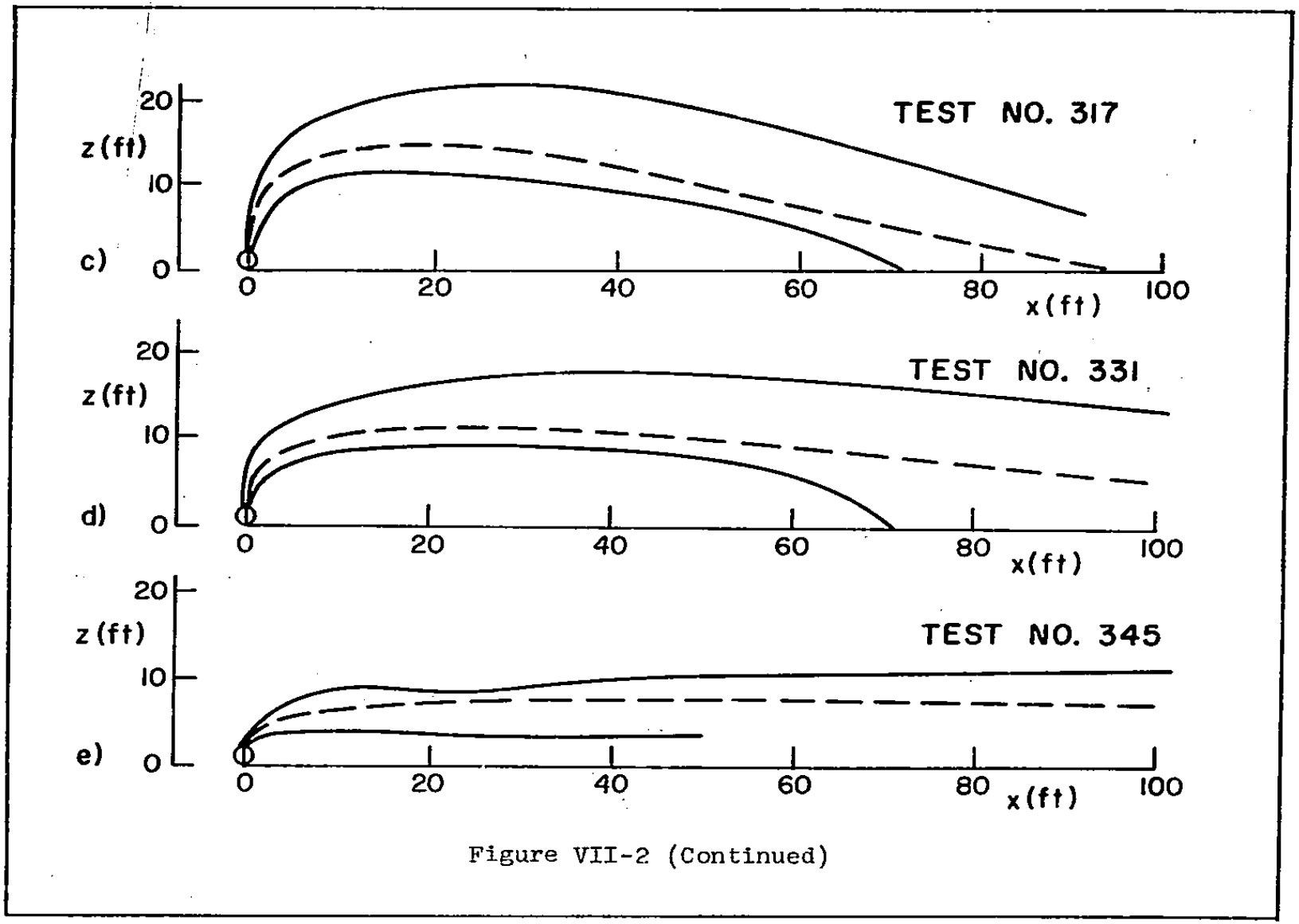

Figure VII-2 (Continued)

SECTION VII. APPENDIX C. COMPARISON OF THE NUMERICAL MODEL WITH THE WES FLUME EXPERIMENTS

In this sequence, the x coordinate of the centerline peak increases with increasing F_e, while the z coordinate decreases. The values of xc also increases with increasing F_e. All of these trends are what one would intuitively expect and also are what the experiments show. In this sequence of tests the position of the centerline is much better than it was in the case of increasing F_D. The rising portion of the centerline is again particularly good, while the portion past the peak is much better than for the previous sequence.

In both sets of geometry tests, it should be noted that the portion of the centerline past the peak is nearly a straight line. It seems that it should be curved more, and indeed if it were, its position within the jet boundaries would be improved. Also, the centerline appears to reach its peak before the boundaries do, which again causes its position to be off somewhat.

In comparing predicted dilution distributions with those measured in the WES tests the model was run for all the dilution tests reported in Part I of the WES report. Figure VII-3 is a plot of the observed axial (minimum) dilutions versus the axial dilutions calculated by the model. The dotted line represents a one-to-one, or perfect correlation. Various symbols have been used in plotting the points to indicate different distances downstream from the port. From this figure it can be noted that the calculated dilutions generally exceed the observed dilutions, especially for cases of large x, which are all past the jet peak. In general, from this figure it appears that the dilution distributions (like the geometry configuration) is better for the portion of the jet between the port and the peak than it is for the portion past the peak, and probably for the same reasons stated previously.

Figures VII-4 through VII-11 are plots of $(E_o/E - 1)$ versus arc length, s, for the geometry tests listed in Table VII-I (except tests 308 and 310 are not included in these figures). The circle in each of these figures corresponds to the centerline peak. The initial portion of each of these curves is a straight line with a slope of 1.0, therefore for this portion of the jet

$$E = \frac{E_o}{1 + mx} \quad , \qquad \text{(C-1)}$$

where m is a constant.

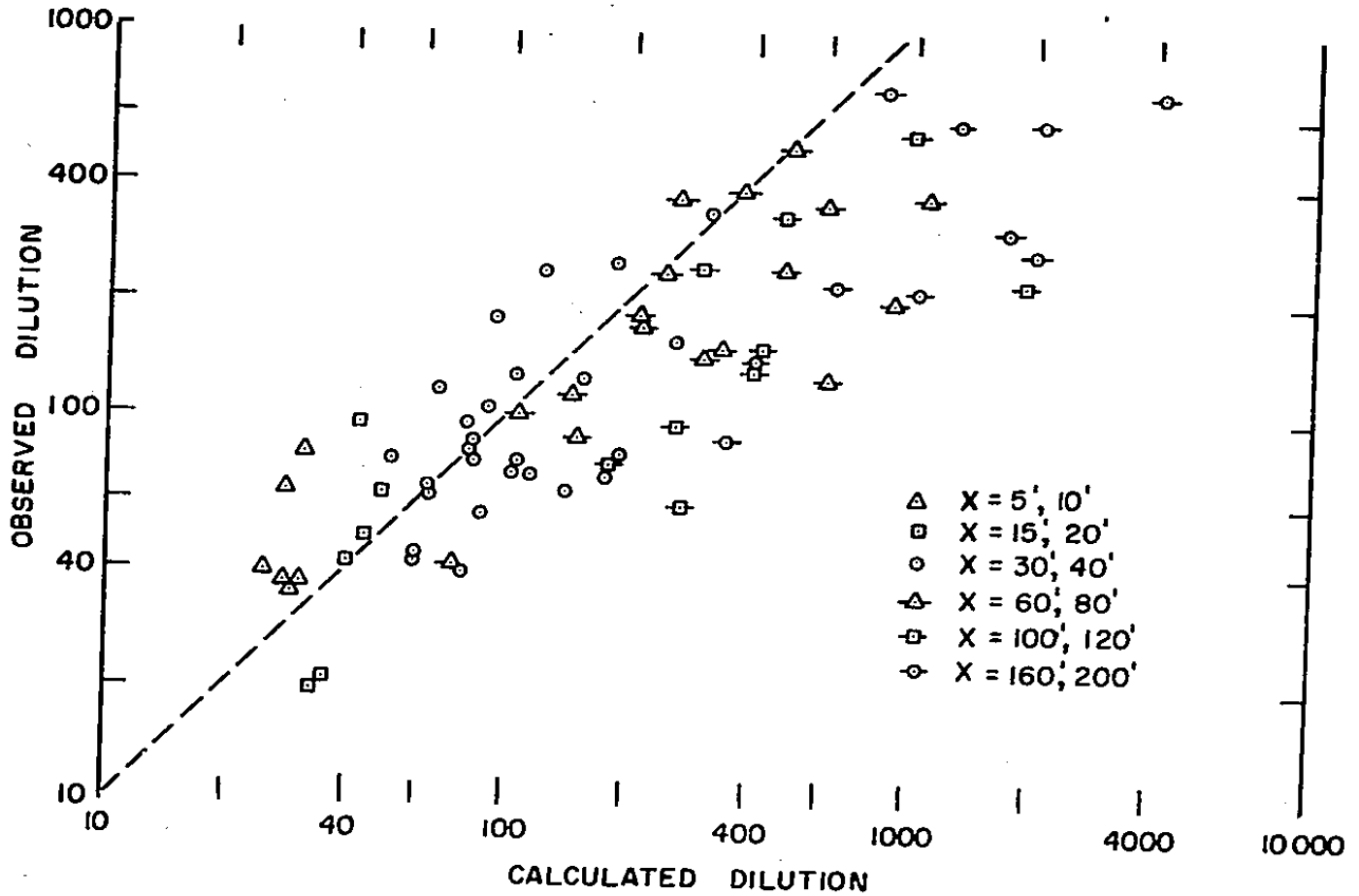

Figure VII-3
Comparison of calculated and observed dilutions.

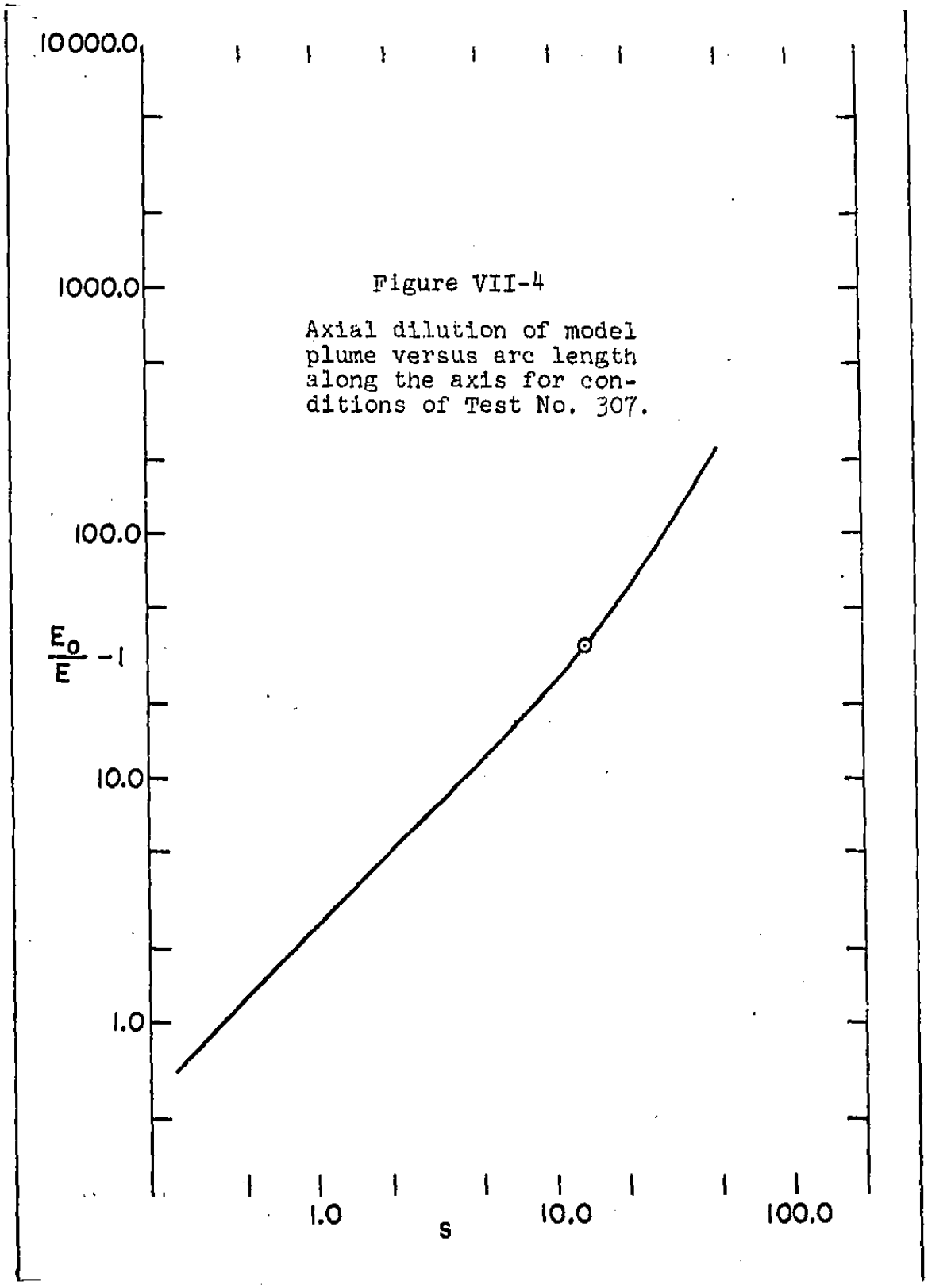

Figure VII-4

Axial dilution of model plume versus arc length along the axis for conditions of Test No. 307.

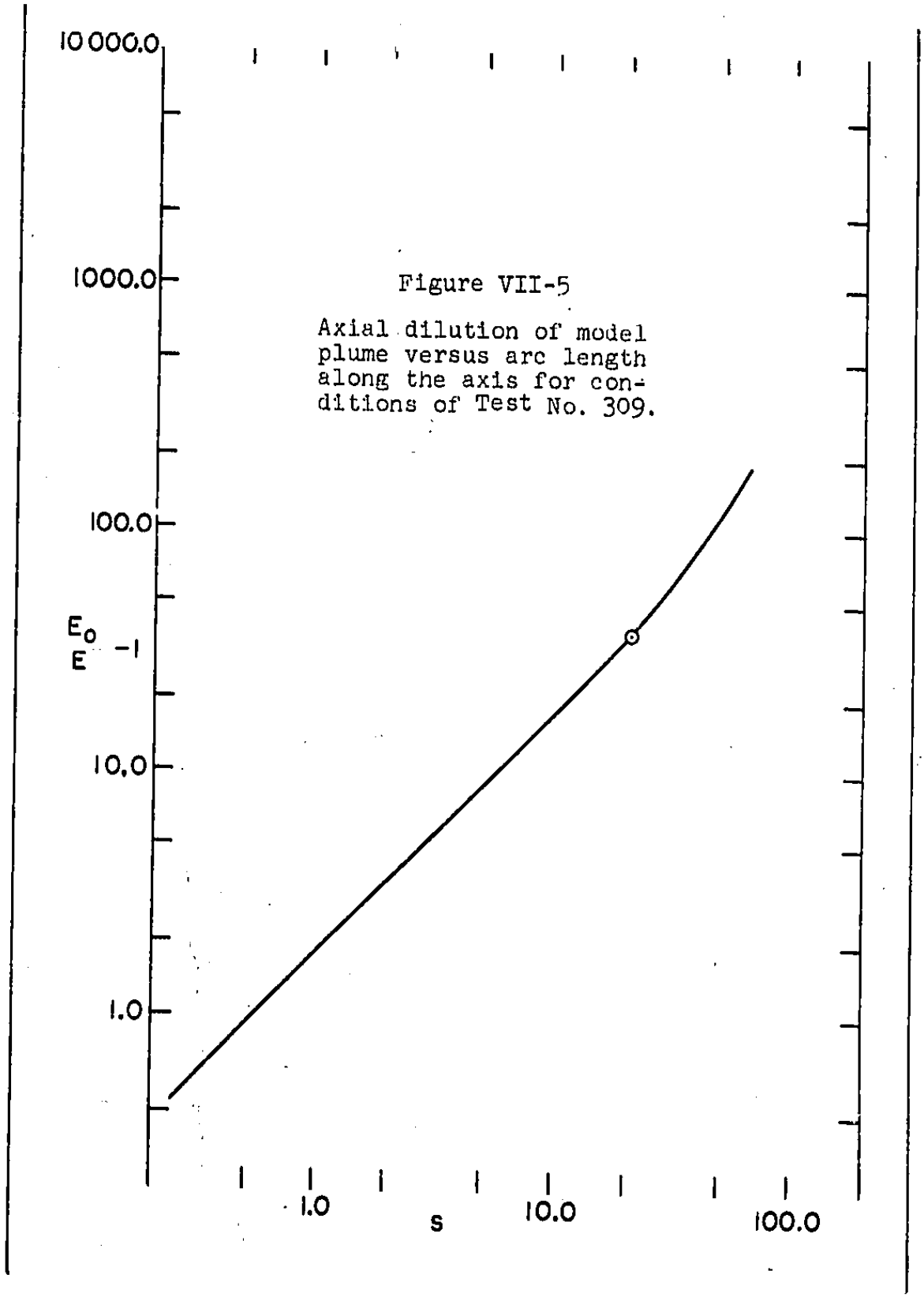

Figure VII-5

Axial dilution of model plume versus arc length along the axis for conditions of Test No. 309.

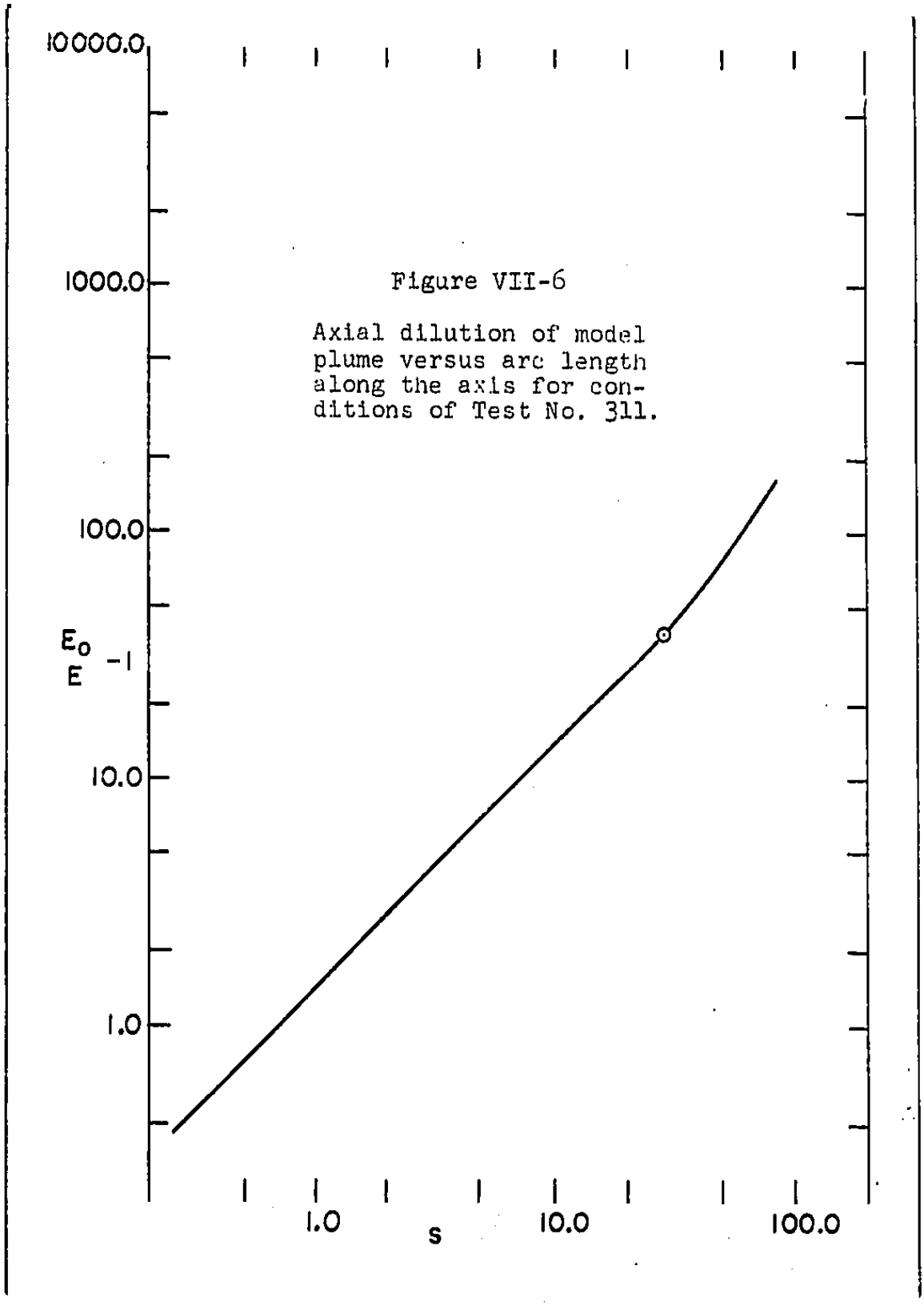

Figure VII-6

Axial dilution of model plume versus arc length along the axis for conditions of Test No. 311.

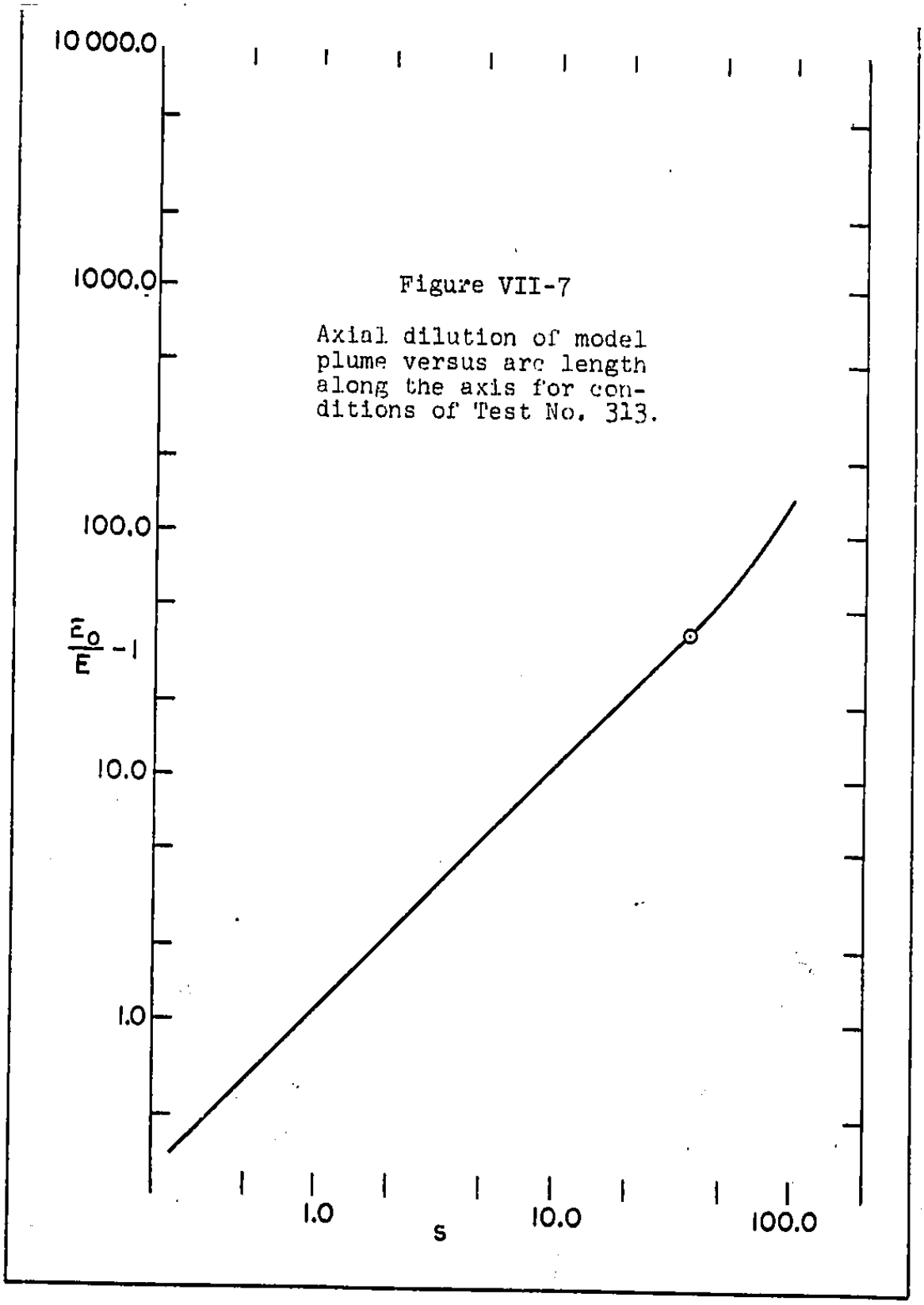

Figure VII-7

Axial dilution of model plume versus arc length along the axis for conditions of Test No. 313.

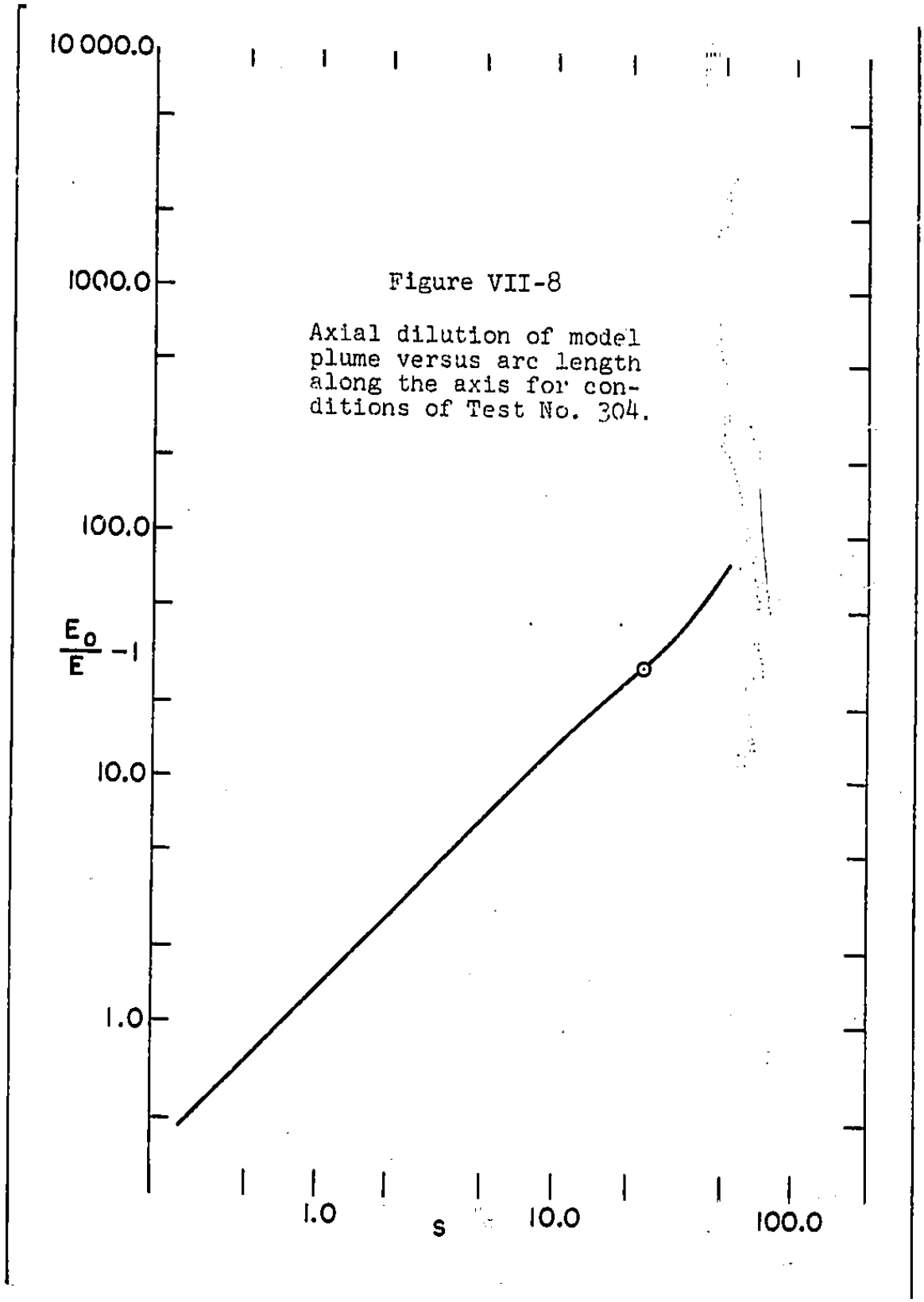

Figure VII-8

Axial dilution of model plume versus arc length along the axis for conditions of Test No. 304.

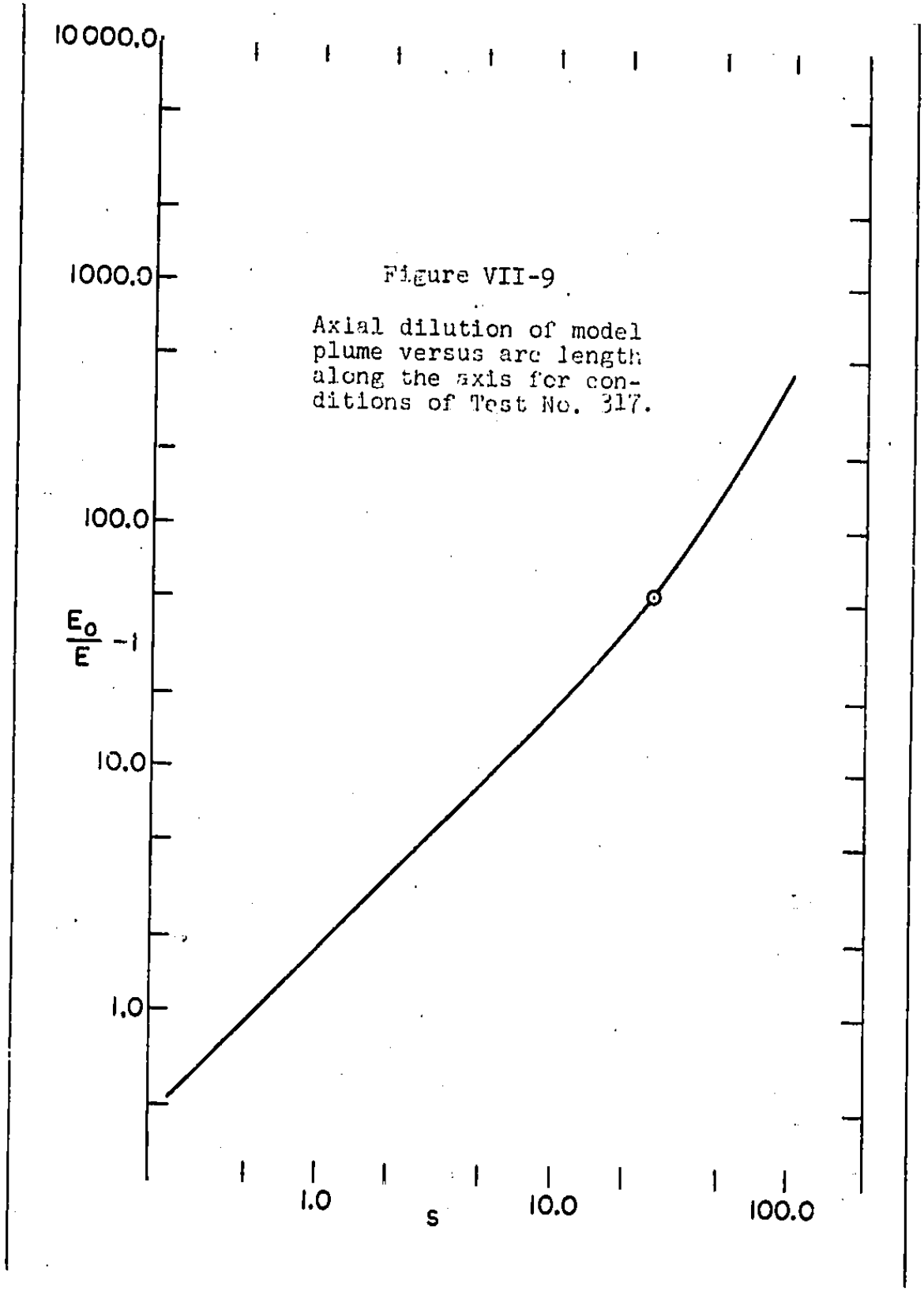

Figure VII-9

Axial dilution of model plume versus arc length along the axis for conditions of Test No. 317.

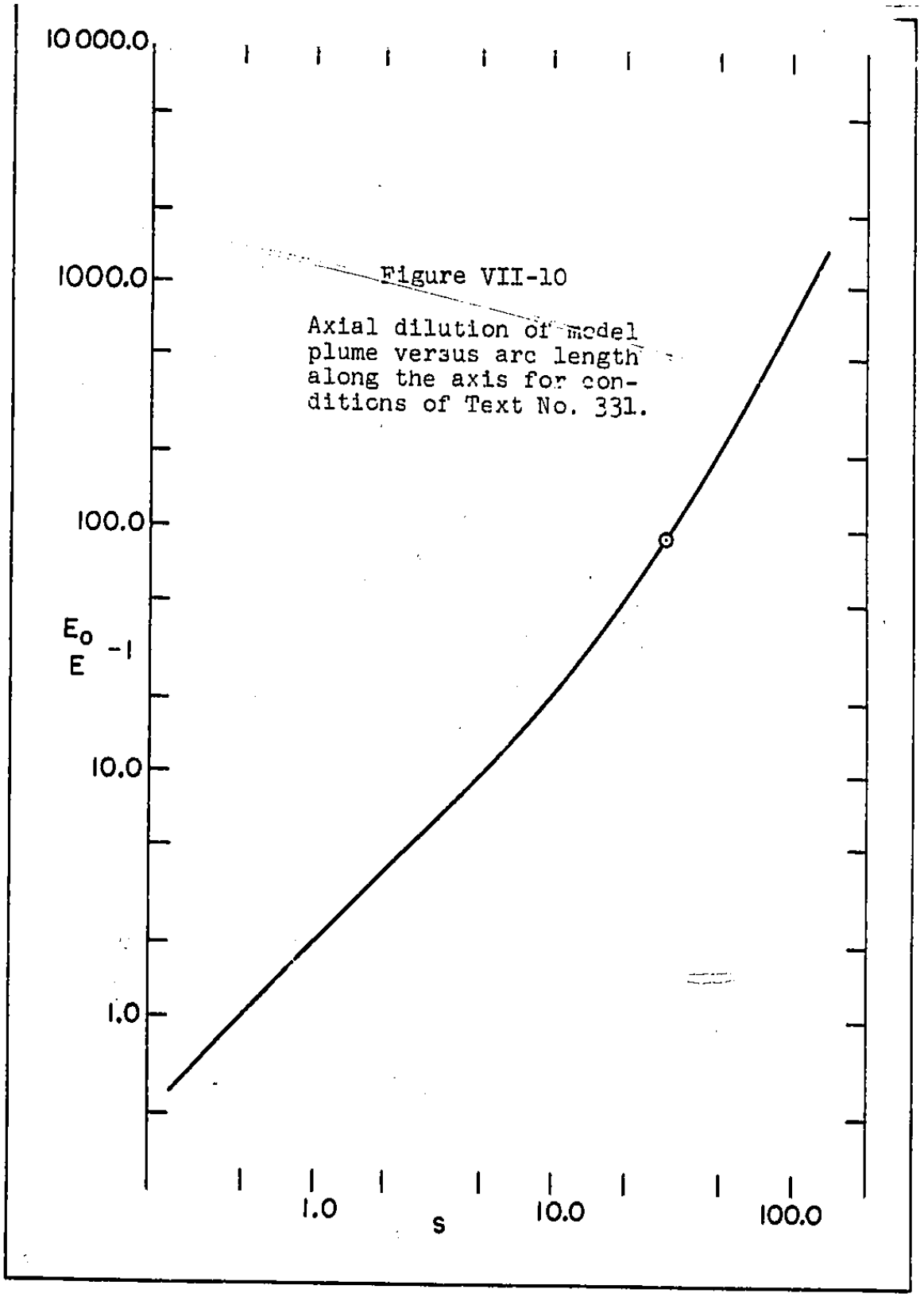

Figure VII-10

Axial dilution of model plume versus arc length along the axis for conditions of Text No. 331.

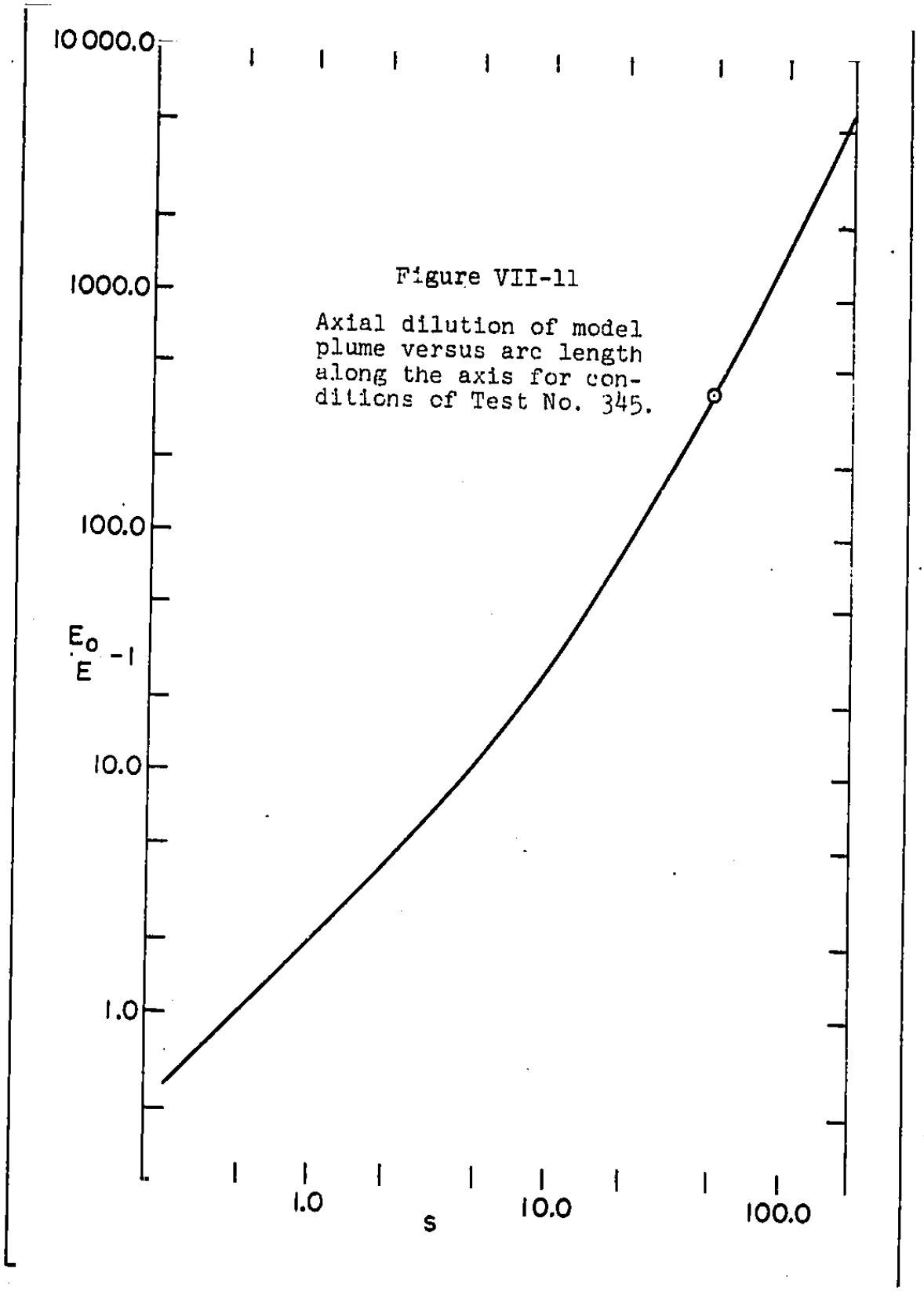

Figure VII-11

Axial dilution of model plume versus arc length along the axis for conditions of Test No. 345.

SECTION VII. APPENDIX C. COMPARISON OF THE NUMERICAL MODEL WITH THE WES FLUME EXPERIMENTS

For values of F_e less than 1.0 (and over the range of $18.8 \leqslant F_D \leqslant 52.2$), the straight line portion of these curves generally extends to the centerline peak, so at least over these ranges of F_D and F_e, axial values of dilution in Figure VII-1 (provided, s, is known).

Figures VII-4 through VII-7 are for the increasing F_D (constant Fe) sequence of tests. For a given values of s, it can be seen that the dilution, $(E_o/E - 1)$, decreases with increasing F_D. This is to be expected since the entrainment coefficient, α, as calculated by (36) decreases with increasing F_D.

Figures VII-8 through VII-11 are for the increasing F_e (constant F_D) sequence of tests. For a given value of s, it can be seen that the dilution increases with increasing F_e. This is also to be expected since α increases with increasing F_e.

From the foregoing discussion it appears that the relationship for the entrainment coefficient, α, and possibly the relationship for λ need to be modified in order to effect better correlation between the model and experimental results. The entrainment relationship needs to be modified so that when the jet direction is reversed (after passing the peak), entrainment is inhibited. This should help correct the scatter shown in Figure VII-3 especially for the points far downstream from the port. As has been indicated previously, the model overestimates the lateral spreading factor by a factor greater than two. Decreasing the dilution should help correct this effect also.

The x coordinate of the centerline peak, X_{am}, needs to be increased in most cases. The z coordinate, Z_{am} appears to be reasonable. If the relationships for α and λ can be modified so that X_{am} is increased, then the effect of decreased dilution should help the geometry correlation by increasing the curvature of the centerline and causing it to fall more rapidly.

It should be emphasized that X_{am} must be increased in order to prevent any decreased dilution from having an adverse effect on the geometry correlation. In the geometry tests where $F_D > 35$ (all tests shown except 307, 308, 309), the centerline already appears to fall too rapidly. For these cases, decreasing the dilution without increasing X_{am} would make the correlation poorer.

SECTION VII. APPENDIX C. COMPARISON OF THE NUMERICAL MODEL WITH THE WES FLUME EXPERIMENTS

For the portion of the jets past the peak, the combined effect of any new relationships for α and λ should be threefold: (1) decreased dilution; (2) increased X_{am}; (3) increased curvature of the jet axis. Any future work on the dense jet problem should begin by working on these relationships.